6-4-1962

An Analysis of the Origins and the Effects of Corporate Financial Policy in a Small Manufacturing Firm

Robert W. Meyer

A STUDY OF TEMPERATURE MEASUREMENT PRECISION IN DEBYE-SCHERRER SPECIMENS DURING HIGH TEMPERATURE X-RAY DIFFRACTION MEASUREMENT OF THERMAL EXPANSION

by

Roy Glenn Merryman

A Thesis

Submitted in Partial Fulfillment of the

Requirements for the Degree of

Master of Science in Mechanical Engineering

The University of New Mexico

1962

Grad Off

This thesis, directed and approved by the candidate's committee, has been accepted by the Graduate Committee of the University of New Mexico in partial fulfillment of the requirements for the degree of

MASTER OF SCIENCE

Stewart A. Northrop
Dean

June 6, 1962
Date

Thesis committee

Victor J. Skoglund
Chairman

Charles P. Kempter

R. C. Dove

ACKNOWLEDGMENTS

The author wishes to thank Dr. C. P. Kempter and Dr. Victor J. Skoglund for their excellent guidance and valuable suggestions in the direction of the work of the thesis as Advisor and Thesis Committee Chairman, respectively.

Appreciation is expressed to L. A. Wahman for his valuable assistance in the laboratory work, to Dr. D. P. MacMillan and Dr. J. D. Rogers who made the thesis project possible, to J. T. Simmons, H. C. Lauf, J. E. Runyan, and their co-workers, and G. H. Whitehead, H. Filip, A. R. Lujan and C. E. Landahl for assistance with the apparatus, to Dr. R. K. Zeigler and his co-workers for the least squares analyses and Dr. W. L. Sibbitt, Dr. T. P. Cotter, Dr. D. G. Rose and all other members of N-Division who may at one time or another have been consulted on this work. I am especially indebted to Mrs. Elizabeth Kennedy for her work in preparing the manuscript.

The thesis was completed in the Los Alamos Scientific Laboratory's training program in cooperation with the University of New Mexico.

TABLE OF CONTENTS

ILLUSTRATIONS

TABLES

APPENDICES

INTRODUCTION

From the advent of the Atomic Age to the present there has been an increasing demand for materials to withstand high temperatures. Properties such as corrosion resistance, low thermal stress, compatibility, strength retention, and fabricability are important considerations in the quest for such materials.

Thermal stresses are proportional to the coefficient of linear thermal expansion. The importance of thermal stress and its relation to thermal expansion in the design of nuclear reactors operating at high temperatures prompted this investigation. Thermal expansion data at temperatures above 1000°C were seldom found, while data which might be extrapolated were in most cases found to be in disagreement among the various authors so that extrapolating was unreliable.

One of the methods for measuring thermal expansion uses X-ray diffraction to give lattice parameters which can be translated to thermal expansion. One of the appealing features of this method is the small quantity of material required which is on the order of 10^{-4} cc. This means that the feasibility of using the material in reactor design from the standpoint of thermal expansion can be evaluated before expensive production facilities are developed.

The X-ray diffraction method is very precise where the lattice measurements are concerned. However, temperature measurements have not been as precise, and consequently the thermal expansion coefficients have been uncertain, and especially so when they have been extrapolated.

It was the purpose of this investigation to determine as precisely and directly as possible the temperature of the Debye-Scherrer specimen in the X-ray diffraction measurement of thermal expansion to 1000°C. It is assumed that the methods developed could be applied in principle at higher temperatures.

From the outset, the temperature would be measured so that the only uncertainties would be those of instrumentation, which with due care are relatively small. It was also anticipated that more than one approach could be evolved for purposes of cross checking.

During the course of the investigation, an invitation was extended by the Bureau of Mines at College Park, Maryland, to participate in an international program of measuring the thermal expansion of a common sample of MgO. This provided an excellent opportunity for evaluating the quality of results by comparison with other investigators.

LITERATURE

The literature cited covers a comprehensive survey on temperature measurement methods in thermal expansion determination utilizing X-ray diffraction from 1921 through 1961 and a compilation of all published data on the thermal expansion of gold from 1916 through 1960 and magnesium oxide from 1906 through 1961. References for comparison of the MgO results with those of the Bureau of Mines Interlaboratory Program of Thermal Expansion Measurements on MgO are also presented. The literature on temperature measurement was limited to those articles featuring camera design or temperature conditions, since to examine publications on all phases of thermal expansion was found to be beyond the scope of this work. The references are presented in chronological order under the headings of Temperature Measurement and Thermal Expansion Measurements on Gold and Magnesium Oxide.

Temperature Measurement in Thermal Expansion by X-ray Diffraction

It appears that the first experiments in high temperature X-ray diffraction were done by Westgren[1] in 1921 using a Debye-Scherrer camera with wire specimens heated by passing a current through them. Similar methods were used later by Becker[2] and Cohn[3].

Jay[4] developed a high temperature X-ray camera in which the temperature calibration consisted of measuring the known lattice parameters of silver to give temperature which was in turn plotted against furnace power and was said to be "probably accurate to 3°C." He did not use a thermocouple because he claimed (1) it was difficult to place at specimen position, and (2) conduction of the leads result in thermocouple temperature lower than the sample.

Dorn and Glocker[5] developed a high temperature camera and made an effort to eliminate Jay's objections to thermocouples. They placed the thermocouple on the furnace core and calibrated by observing the melting point of standard materials in the sample position. The furnace temperature at the thermocouple was stated to be held to $\pm$ 2°C, but there was no comment on the precision of the sample temperature. The maximum temperature was 500°C.

Hume-Rothery and Reynolds[6] described a high temperature camera used in the study of the lattice spacing of silver. Temperature was measured with a movable ring thermocouple in the furnace. Specimen temperature was obtained by (a) measuring the temperature in the mouth of each section of the furnace, upper and lower; (b) then measuring the temperature at the center of the gap, giving a "centre-point drop"; (c) during the run, the thermocouple is withdrawn to the edge of the gap out of the X-ray beam, and is used to control the furnace temperature to $\pm$ 0.5°C by hand; (d) specimen temperature is assumed to be that of the ring thermocouple when located at the center of the gap, e.g., the mean temperature recorded during exposure is corrected for "centre-drop". The only reference to precision of the measurement was "it is improbable that the temperature of the specimen and thermocouple differed by more than 1°C."

Ellwood[7] made a study of aluminum-zinc alloys using a new camera design. The camera was 20 cm in diameter, and used an iron-constantan thermocouple which was calibrated before and after an experiment (presumably by comparision with a standard). The thermocouple was 1 mm from the specimen, and there was a 1/2°C drop to center of gap. It was stated that pictures vere obtained in from 45 minutes at room temperature to 3 hours at 450°C.

(This is surprising because our smaller camera (19 cm) with a silver specimen required from 10 hours at room temperature to 30 hours at 900°C.) The accuracy was "estimated" to be ± 2°C at 450°C.

A. J. C. Wilson[8] measured the thermal expansion of aluminum using a camera patterned after the Jay (1933) and H-R and R (1938) models. The furnace was operated to 1000°C using the ring type thermocouple described in Hume-Rothery's paper. The furnace temperature varied about 1°C, and it was "thought" that the temperature measurements were reproducible within 0.5°C and were within 1°C of the International Temperature Scale. He found the "centre-drop" of temperature in the furnace to disappear with the use of aluminum foil radiation shields.

Birks and Friedman[9] described a diffractometer used to 1200°C in vacuum. The sample temperature was maintained to ± 5°C. Do details were given as to the method of measurement or its precision.

Another diffractometer was made by Van Valkenburg and McMurdie[10] for use to 1500°C. The furnace temperature was controlled to ± 1°C. (There was no reference to sample temperature, nor to temperature gradients in the sample which are known to exist.)

Alcock, Peiser, and Swallow[11] designed a high temperature powder camera utilizing two sets of coaxial platinum-rhodium hemispheres for radiation shielding to attain better vacuum (ceramic insulation in most furnaces is ahindrance in high vacuum work due to its outgassing). The maximum temperature was 900°C. Temperature was derived from (a) the resistance of the furnace windings, or (b) from the pattern of a fine platinum wire wound around the sample. No precision of the temperature measurement was stated.

Gordon[12] modifed a back-reflection symmetrical focusing type camera and used a resistance furnace with a platinum winding. Vacuum was in the range of 5×10^{-6} mm Hg. Temperature was measured with a thermocouple in the sample holder. The thermocouple was calibrated against another thermocouple placed on a dummy sample; the difference found was less than $5^{\circ}C$ up to $1000^{\circ}C$.

Edwards, Speiser, and Johnston[13] designed an induction heated powder camera using vacuum or inert gas. The sample temperature was obtained from the average of the upper and lower furnace temperature readings which had previously been calibrated by observing the melting points of various metals with a pyrometer. It was stated that lattice parameters calculated from back reflections were obtained with an accuracy of 0.02% or better.

Goldschmidt and Cunningham[14] designed a camera to operate to at least $1400^{\circ}C$ in a vacuum or gas. A movable thermocouple was used to measure the temperature by moving it into the vicinity of the sample before and after exposure (similar to Hume-Rothery's method). No error was discussed. The camera had exchangeable slits used for increasing exposed specimen height to overcome the problem of grain growth and to shorten exposures.

Williams[15] developed a high temperature camera for the Debye-Scherrer examination of flat solid specimens using a side reflection technique. Sample temperature was measured to over $1000^{\circ}C$ with a thermocouple in contact with the specimen. The "accuracy" of Al and Cu lattice parameters to $610^{\circ}C$ and $900^{\circ}C$, respectively, was 1 in 50,000. It was stated that the sample thermocouple and temperatures derived from lattice parameters agreed with the limits of accuracy of the instrument.

Mueller and Zauberis[16] describe a camera for high temperature X-ray diffraction using radio frequency for heating. They claim the sample temperature to be held constant to at least ± 0.2% from a thermocouple in the eddy current field. It does not say what the ± 0.2% refers to, but probably the temperature at time of reading. The sample temperature is obtained from a calibration of furnace power against a pyrometer and materials of known melting point. No figure is given for the precision of sample temperature.

Berry, Henry, and Raynor[17] explored the temperature field in the furnace gap of an early Unicam camera, one with cylindrical cavities in top and bottom furnace halves. Both furnace sections were separately controlled at the same temperature to ± 0.1°C. The temperature gradient over the gap was found to be ± 2.25°C at 200°C and increased to ± 5.5°C around 550°C. An emissivity error of as much as 20°C at 500°C was observed and increased with temperature. They feel that temperature measurements in the gap are unreliable unless the thermocouple is attached to the specimen.

Basinski, Pearson, and Christian[18] modifed the Unicam thermocouple arrangement by using 5 mm diameter ring type thermocouples around the specimen, one in the mouth of the upper furnace half and one in the mouth of the lower half. Each half of the furnace, which has been modified to a spherical cavity, was controlled separately. Results were said to be reproducible but no precision was stated. With a Ag calibration in the 700-930°C range, thermocouple readings were said to agree within 2°C with the H-R silver data.

Mauer and Bolz[19] measured the thermal expansion of tungsten in a diffractometer. They used both a chromel-alumel thermocouple on the edge of the sample and an optical pyrometer, where possible, and found the two

methods differed by as much as 60°C. (This may be due to emissivity of sample.)

Birks[20] made some diffraction studies of metals in which the film was replaced with a Geiger counter (diffractometer method). Temperature was obtained from a Pt/Pt -10% Rh thermocouple welded to the sample.

Johnson[21] designed a high temperature camera in which the sample was heated with tantalum strips in vacuum. A pyrometer was used for temperature measurement. Calibration to give sample temperature was obtained from reading a rod of the sample material larger than the specimen with a hole drilled to give a black body temperature. This temperature was compared with the surface temperature as would be read on the specimen to give a true sample temperature. The maximum temperature was 2200°C.

Pease[22] made a theoretical and experimental examination of specimen temperature in a 19 cm Unicam high temperature camera with cylindrical furnace halves. The thermocouple was in the mouth of the top half above the specimen. He found errors of opposite sign which increased to a maximum at about 200°C and then decreased with increasing temperature which he attributed to conduction through the thermocouple leads. The error was zero at about 600°C, after which the error again increased but with opposite sign with the geometrical error predominating over the conductive error. Observations were made to 800°C and under 5 microns of vacuum.

E. Matuyama[23] constructed a 20 cm diameter camera for measuring the thermal expansion of graphite from 1000 to 1800°C. The temperature was measured with a pyrometer. The specimen temperature was said to be 20° lower than the surface of the graphite heating element at 1000°C and 40° at 1800°C. It is said "the furnace temperature remained sufficiently constant

over the entire exposure of eight hours." (No exact figures of "sufficiently constant" were given. Since measurement was with a pyrometer, it is assumed the accuracy was probably no better than $\pm$ 5°C.)

Mauer and Bolz[24] measured the thermal expansion of cermet components to 1400°C obtaining the temperature with a thermocouple on the edge of the sample in a diffractometer. This thermocouple was calibrated using the silver lattice data on Hume-Rothery (1938). "Accuracy" was estimated to be $\pm$ 3°C.

Basinski and Hume-Rothery[25] measured the lattice spacing of iron. Temperature was obtained from ring thermocouples mounted in the mouth of each furnace half. Calibration was made with two melting points, antimony and silver.

Brand and Goldschmidt[26] produced as uniform temperature as possible by using two hemispherical furnace halves. This is the basis of design for the Unicam camera used in this thesis. In the use of this furnace, they found that "one of the most important (basic problems) is that of accurate measurement of the powder specimen temperature." They suggest methods of calibrating the camera to give a more accurate sample temperature than had been attained before by measurement of materials of known expansion coefficients versus thermocouple temperature. Silver was used up to 900°C, while platinum and tungsten served for the higher temperatures. They cited the following effects on calibration:

1) difference in emissivity between specimen and thermocouple
2) selective loss of platinum or rhodium from the platinum-rhodium leg of the thermocouple through vaporization

3) diffusion of rhodium into the platinum leg of the thermocouple

4) contamination of the thermocouple by material from the specimen

5) conduction of heat along the thermocouple wire

Suggested ways of reducing the temperature correction in the calibration are: (1) increasing diameter of thermocouple weld; (2) reducing diameter of thermocouple wire; (3) improving emissivity of thermocouple bead; and (4) various geometrical shapes of the thermocouple.

Other methods of arriving at sample temperature were briefly described and consisted of the following:

1) calibration by power input

2) calibration by melting points

3) calibration by transition points

4) internal calibration - mixing material of known thermal expansion with sample

5) optical pyrometer

Expansion equations are given for materials that can be used in calibration work - Ag, Pt, Au, Cu, Al, and W.

Kuznetsov[27] studied the thermal expansion of silver and compared his results with Hume-Rothery (1938). The maximum deviation of the lattice parameters from the H-R data was 0.0009 $\mathring{A}$. He used a semi-ring type thermocouple, 3 mm diameter, which was 1 to 1-1/2 mm from the sample. The error claimed was 1-2°C.

Zimmerman and Allen[28] measured the thermal expansion of refractory crystals with a back reflection camera. Measurements were made to 1200°C, and "the specimen temperature could be maintained plus or minus 3°C during an entire exposure." The thermocouple appears to be on the back of the specimen holder.

Fridrichsons[29] described an adapter to provide a heat source for cameras not so equipped. Internal standards of Ag or Pt were used to obtain temperature indication. Maximum temperature was 1000°C.

Austin, Richard, and Schwartz[30] designed a camera for temperatures to 2000°C and a vacuum to 10^{-6} mm Hg. Low temperatures were read from a thermocouple in the furnace gap next to the specimen while high temperatures were read with a pyrometer. No calibration procedures were given and precision of the sample temperature was not stated.

Skinner[31] investigated the thermal expansion of thoria, periclase, and diamond, using a back reflection camera of 16 cm diameter. Temperature was read from a movable thermocouple 1/32" from the specimen and at 60° (angle) intervals around the sample. It is stated that the temperature, presumably of the sample, was held to $\pm$ 1°C at 400°C for 48 hours with a variac and constant voltage transformer.

Goon, Mason, and Bigg[32] designed a powder camera for X-ray work at high temperatures and pressures. The sample temperature was "indicated" to be accurate to $\pm$ 3°C. Description of the calibration method was not clear but it is believed that the thermocouple in the furnace was calibrated aginst the lattice parameters of silver.

Gindin and Prokhvatilov[33] described a device for high temperature X-ray work in which the specimen was applied onto a 0.2 mm platinum wire which is heated by passing current through it. The method and accuracy of temperature measurement was not given. This appears to be similar to that described by Westgren in 1921.

Hanak[34] in a study of rare earth allotropy, calibrated the furnace of the camera using the silver lattice data of Hume-Rothery.

Aruja, Welch, and Gutt[35] developed a technique in which the sample was coated on the thermocouple. A unique feature of this system was the power and thermocouple signal being transmitted on the same wires. The system was limited to non-conductors, and the accuracy of the temperature measurement was "guessed" at $\pm$ 10°C.

Spreadborough and Christian[36] designed a vacuum furnace which could be used with a commercial diffractometer. It was operated up to 1100°C, and it was believed higher temperatures could be achieved. The sample temperature was stated to be "controlled by hand to $\pm$ 2°C" from a thermocouple in the holder. The true specimen temperature was claimed to be "close" to the thermocouple reading because of agreement with the silver lattice data of Hume-Rothery.

Van Niekerk[37] described a vacuum furnace for a diffractometer in which temperature measurement was obtained from a furnace thermocouple near the sample holder calibration against a "standard thermocouple" embedded in a powdered quartz specimen, giving a plot of furnace thermocouple millivolts versus sample temperature. Comparison with known values of phase changes for quartz and iron indicated a precision of $\pm$ 2 to 4°C.

Simmons and Balluffi[38, 39] studied the equilibrium concentration of lattice vacancies in silver and aluminum. The back-reflection rotating-single crystal technique was used. It is stated "the high thermal conduction of the specimen and graphite insured that the actual specimen temperature was measured" where the thermocouple was in the graphite sample holder 3 mm from the sample.

Das[40] developed a high temperature X-ray diffractometer for use up to 2000°C in a vacuum of 10^{-6} mm Hg. Beryllium windows (.010") were used. Temperature was read directly with a Leeds and Northrup pyrometer when possible and, when the viewing window became fogged, a power calibration was used.

Intrater and Hurwitt[41] developed an attachment for the Norelco diffractometer for high temperature, high vacuum work. They say "a critical problem of high temperature operation is measurement of specimen temperature." The attachment is good to 1500°C and stable to ± 2°C. The sample is mounted on a Pt-40% Rh ribbon which also forms the furnace element. Optional methods are given for finding a sample temperature such as a thermocouple on the heater element, calibration of pyrometer or furnace current with melting point standards, or internal standards mixed with sample. No error or accuracy is given for sample temperature.

Current Work

At the Tenth Annual Conference on Applications of X-ray Analysis held in Denver, Colorado, August 1961, which the author attended, several papers recognizing the problem of specimen temperature in high temperature X-ray diffraction were presented. No current reference, however, has been found devoted exclusively to temperature determination.

Mauer and Bolz described a high temperature mount for the back reflection region for the diffractometer. The maximum temperature was 1400°C. With an optical pyrometer and by mounting the thermocouple in various locations of the sample, gradients as high as 50°C at 1200° were found, and variations in the X-ray beam area were about 20°C. From melting point and lattice parameter "standards", the thermocouple correction was +36°C. These variations were found to be dependent on the character of the specimen also. Changes in design are being considered to improve this situation.

Campbell and Grain studied the expansion characteristics of alumina to 1200°C. Errors were considered less than 3% above 500°C, and about 2% at 1000°C. This work was previously published (42) and included measurements on MgO.

Vaughan and Schwartz described the temperature measurement and control in connection with thermal expansion work on uranium, uranium dioxide, and magnesium oxide.

Corvin et al developed an attachment for high temperature diffractometry to observe chemical reactions with vapors to 900°C. The constancy and distribution of temperature over the sampling area were determined.

Thermal Expansion of Gold

Muller[43] used the method of Fizeau (interferometer). For the range of 0-520°C, he gave

$$\frac{l - l_o}{l_o} \times 10^6 = 14.157\ t + 0.002150\ t^2$$

from which the values were calculated for comparison.

Austin[44] used an interferometer with the specimen in vacuo to measure the expansion of gold from 0° to 900°C. The data were converted to 25°C reference using ratios derived from equations in this thesis for the purpose of comparison.

Shinoda[45], using X-ray diffraction, placed the gold sample on the tungsten filament. Temperature was determined from the change in resistance of the filament. No precision was given for the temperature.

He found the following value for gold:

$$\alpha_{mean}(15\text{-}500^\circ C) = 13.2 \times 10^{-6}/^\circ C$$

from which the percent expansion was calculated for comparison. Cu Kα radiation was used. No details of calculation methods were given.

Fizeau[46] with an interferometer found the expansion coefficient for gold

$$\alpha \text{ for } 0\text{-}100^\circ C = 0.0000144/^\circ C$$

Esser, Eilender and Bungard[47] used X-ray diffraction to find the thermal expansion of gold. The Debye-Scherrer method was used and the temperature appeared, from translation of the German, to have been measured from a thermocouple spot welded to the specimen. Details were requested from the author (Bungard) and he confirmed that this interpretation was correct. Data points are taken from an enlargement of the curve given in the report and, after conversion from kX to Å units, used in the comparison.

Nix and MacNair[48] made extensive dilatometer measurements on gold from -187.0°C to 720.8°C at close intervals of from 1° to 13°C. Selected values from a plot of the data and adjusted to 25°C reference are used in the comparison.

Esser and Eusterbrock[49], using the dilatometer method, measured the expansion of gold from 0°C to 950°C. Selected values adjusted to 25°C reference are used for the comparison.

Gott[50] used X-ray diffraction with both a thermocouple and an internal standard of Al for temperature measurement. Calculation was by the "last lines" method. Values were taken from a plot of the data for purposes of comparison.

Swanson and Tatge[51] show the following lattice parameters for gold at 25°C by various authors:

	a_o, Å
Sachs and Weerts	4.0785
Owen and Yates	4.0786
Jette and Foote	4.0786
Esser, Eilender, and Bungard	4.078
Swanson and Tatge	4.0786

Krikorian[52] in a compilation of thermal expansion data from unknown references gives the following for gold:

t, °C	Percent Expansion from 25°C
500°	0.73
1000°	1.65
1063°	1.80

Thermal Expansion of MgO

Eastman[53] in a Massachusetts Institute of Technology thesis appears to have made the first thermal expansion measurement of MgO. He used a dilatometer. The data are not used here due to the unusual reference temperature (120°C) seen in his equation below.

$$\alpha_t = 10^{-8} [1140 + 0.92 (t - 120^\circ)]$$

Rieke[54] used the dilatometer method to measure the MgO expansion up to 700°C.

Bogitch[55] made dilatometer measurements on magnesia (88% MgO). His data for comparison were read from a curve in the reference.

Thilenius and Holzmann[56] used the dilatometer method on MgO specimens. The percent expansion for comparison was calculated from selected values of their linear expansion coefficients and plotted to obtain the values shown.

Kanz[57] determined the expansion of MgO with a dilatometer and found the values used directly in the comparison up to 1000°C.

Austin[58] used a modified interference method in which the "accuracy" of results was "believed" good to ± 1% or better. The percent expansion of MgO for comparison was calculated from the linear coefficients given.

Heindl[59] used the dilatometer to measure periclase which was "mostly MgO". The results are used directly in the comparison.

Bussem[60] used X-ray diffraction with a flat plate back reflection camera geometry. The temperature range was -173° to 1300°C from a thermo-

couple located about 2 mm from the irradiated volume of the MgO preparation. Lattice parameters were calculated by taking the average of the a values calculated from the high angle CuKα_1, α_2, and β lines. Values of percent expansion were calculated from the given lattice parameters, and the values shown corresponding to common temperatures for comparison were obtained from a plot of original values.

Ebert and Tingwaldt[61] measured the expansion of magnesia in air to 2000°C with a dilatometer. Their data were converted from 0°C to 25°C reference for the comparison.

Durand[62] made expansion measurements on magnesium oxide to 480°K (207°C) with an interferometer. His data were converted from 0°C to 25°C for the comparison.

White[63] used a dilatometer to measure the expansion of columnar crystals of 96% MgO. His data were used directly for comparison.

Pole, Beinlich, and Gilbert[64] used a dilatometer to measure the expansion of 97.5% electrically fused/2.5% sea water MgO. The data have been used directly in the comparison.

Gangler and Robards[65] made an interferometer measurement of the coefficient of expansion on a hot pressed specimen of MgO, obtaining a value for α (75-1000°F) = 6.94 (in/in)/°F x 10^{-6} (12.5 x 10^{-6}/°C). This was the only point and it fell between the temperatures used for comparison so it was not used.

Sharma[66] used the interferometer method to measure the expansion of a crystal of MgO. The percent expansion values for comparison were calculated from his value for the linear expansion coefficient, and normalized to 100°C, 300°C, etc., from a plot of the data.

Schwartz[67] measured the expansion of a 6-inch sample of "pure MgO" using a telescopic system. Values for the comparison were obtained from his curve of percent expansion versus temperature.

Crandall[68] described a method of expansion measurement used on MgO similar to the interferometer method, but using two parallel line gratings and observing changes in light intensity as one line moves across the other during sample expansion. The curve provided was too small for use in the comparison but is said to compare favorably with Austin's.

Mauer and Bolz[25] used a diffractometer described previously for expansion measurements on a number of cermets. Their data have been converted to 25°C reference and normalized to temperatures of 200°, 400°, etc., for comparison.

Beals[69] measured the expansion of MgO using a back reflection X-ray camera with a thermocouple on the sample holder. Temperatures were normalized to 200°C, 400°C, etc., from a plot of the data but the data were not converted from the given reference temperature of 32°C so appear slightly lower than they should.

Zimmerman and Allen[29] used a back reflection X-ray camera previously described and measured the expansion of a crystal of MgO to 1183°C. Temperatures were normalized to even values of 200°C, 400°C, etc., from a plot of the data for comparison.

Whittemore and Ault[70] used a Gaertner dilatometer. The percent expansion was calculated from the linear expansion coefficient given for MgO for the comparison.

Skinner[32] used a back reflection X-ray camera previously described to measure the expansion of a single crystal of periclase (MgO) to 703°C.

The percent expansion was calculated from the lattice parameters given and then plotted to normalize to even temperatures of 200°C, 400°C, etc., for comparison.

Swanson and Tatge[51] give the following room temperature (25°C) lattice parameters for MgO by various authors:

	a_o, Å
Büssem, Bluth, and Grochtmann	4.211
Straumanis and Ievins	4.2115
Frevel	4.214
Swanson and Tatge	4.213

Engberg and Zehms[71] used a Gaertner dilatometer but the range of their measurements, 1000°C to 2000°C, was above the range of interest for purposes of comparison.

Klein[72] used a diffractometer for measurements of the thermal expansion of alumina and beryllia. MgO was measured to check the temperature calibration of the camera. The MgO data were admittedly not good due to discrepancies found in the temperature measurement, but has been included for comparison. The values were read from the curve given in the report.

Campbell and Grain[42] used two different diffractometers in measuring the thermal expansion of alumina. Measurements on MgO were made to demonstrate the agreement between the two instruments. The data shown for comparison were read from their curve.

Krikorian[52] in a compilation of thermal expansion data lists the following for the percent expansion of MgO:

t, °C	Percent Expansion from 25°C
500	0.61
1000	1.33
1500	2.23
1800	2.82

Since the data are unreferenced, making the method and source unknown, it has not been used for comparison.

The Norton Company[73] in a commercial brochure has listed values of the expansion of MgO, but again references and methods are unknown and the data are not used for comparison.

t, °F	Percent Expansion above 88°F (31°C)
400	0.20
600	0.35
800	0.50
1000	0.65

Fieldhouse and Lang[74] in a report on thermal properties measured the expansion of MgO with a dilatometer. Values were read from their curve of percent expansion versus temperature for the comparison.

APPARATUS

A general view showing the physical arrangement of the apparatus is shown in Figure 1. The regulated DC power supply for the camera furnace is at (A). The vacuum protection circuit is at (B). The Rubicon potentiometer is at (C) which is in the circuit of the Brown millivolt recorder at (D). The Brown recorder for monitoring the output voltage of the DC power supply is at (E). The Rubicon high precision potentiometer and the associated Brown Electronik null indicator for calibration are shown at (G) and (F), respectively. The programmer for controlling the rotation of the sample is shown at (H). The CEC Philips Gauge for measuring the camera vacuum is shown at (I). The Brown (Electronik) controller to adjust for slight drifts in temperature from excursions in room or cooling water temperatures is shown at (J). The Unicam camera assembly is shown at (K). The Norelco X-ray machine is shown at (L). A Sola voltage regulator for the protection of all the instrumentation is shown at (M). Shown but not marked is the CEC diffusion pump located at the top front edge of the X-ray machine and connected to the Unicam camera.

Figure 2 shows a schematic of the apparatus and instrumentation. Letter designations correspond to those in the general view of Figure 1. Items which do not appear in these figures are the Labline tempered water circulator and the Welch vacuum pump used as a fore pump on the camera vacuum system. The Labline water circulator is used to indirectly

control sample temperatures near room temperature by passing water through the camera water jacket, and for this purpose is capable of maintaining the water temperature to $\pm$ 0.02°C.

Figure 3 is a close-up showing the Unicam camera in position at the beam port of the X-ray machine. Figure 4 is a top view of the camera in operating position aligned with the beam. The cassette holding the film is at (A) while (B) is the vacuum chamber. Figure 5 is the same view with the film cassette and lead beam shield removed showing the top of the camera body (C) with the three locating pads for positioning the cassette. When the vacuum chamber is removed, the furnace can be seen at (D) in Figures 6 and 7 with the leads from the furnace thermocouple coming out of the top section. The Pt/Au thermocouple specimen can be seen in the furnace gap of Figure 7. Figures 8 and 9 taken after the final step in disassembly, raising the furnace up and off the camera body, show the specimen in position at (F) on the rotating magnetic holder (E). This happens to be the Pt/Au thermocouple specimen and for illustration the leads are shown connected to the terminals. Actually, the leads are connected after the furnace is in place.

Two typical specimens are shown in Figure 10 with approximately 2X magnification. (A) is a mixture of MgO and Au powders in a silica capillary and (B) is a Pt/Au thermocouple specimen with the junction located in the path of the X-ray beam. The MgO and Au specimen consisted of an approximate mixture of 60% MgO-40% Au powder (-325 mesh) sifted into a 0.010" diameter silica capillary with a wall thickness of about 0.002". This specimen was used to measure the lattice parameters and thermal expansion of MgO. The Pt/Au thermocouple specimen was used to calibrate the Au used

for the temperature standard in the MgO and Au specimen above. It consists of a 0.010" diameter Au wire and a 0.003" diameter Pt wire calibrated by the National Bureau of Standards with a stated accuracy of 1°C. The Pt wire is brazed to the Au wire forming a thermocouple junction in which one leg is also the specimen, i.e. the Au in this case. The thermocouple junction is in the X-ray beam path so errors due to conduction and convection are eliminated. There was no interference from Pt observed in the X-ray diffraction, and when one considers the estimated 1 mil thickness of Au brazing on the junction and the attenuation by Au in Appendix IV, this would be expected.

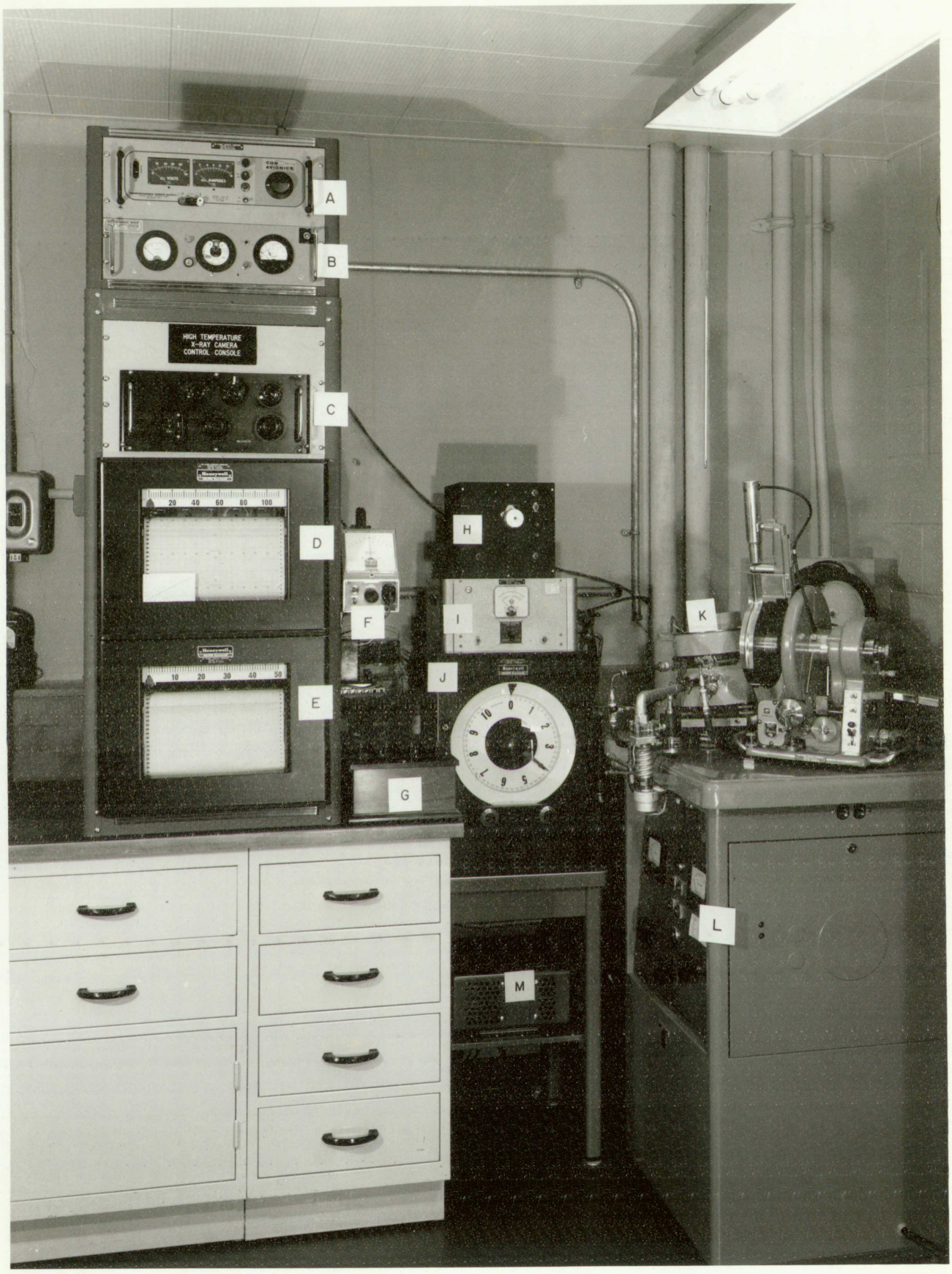

Figure 1. General arrangement of the apparatus.

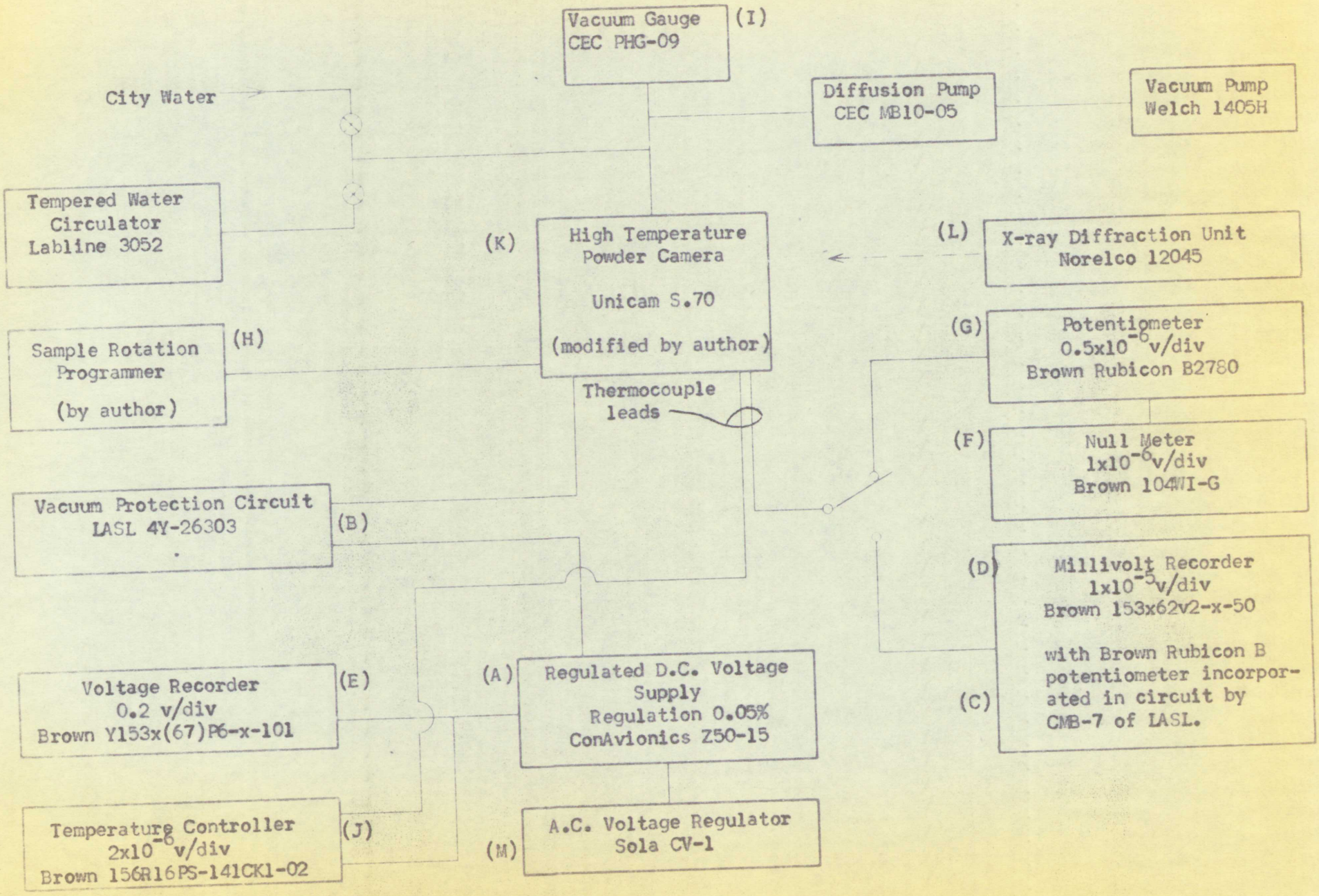

Figure 2. Schematic of Apparatus and Instrumentation

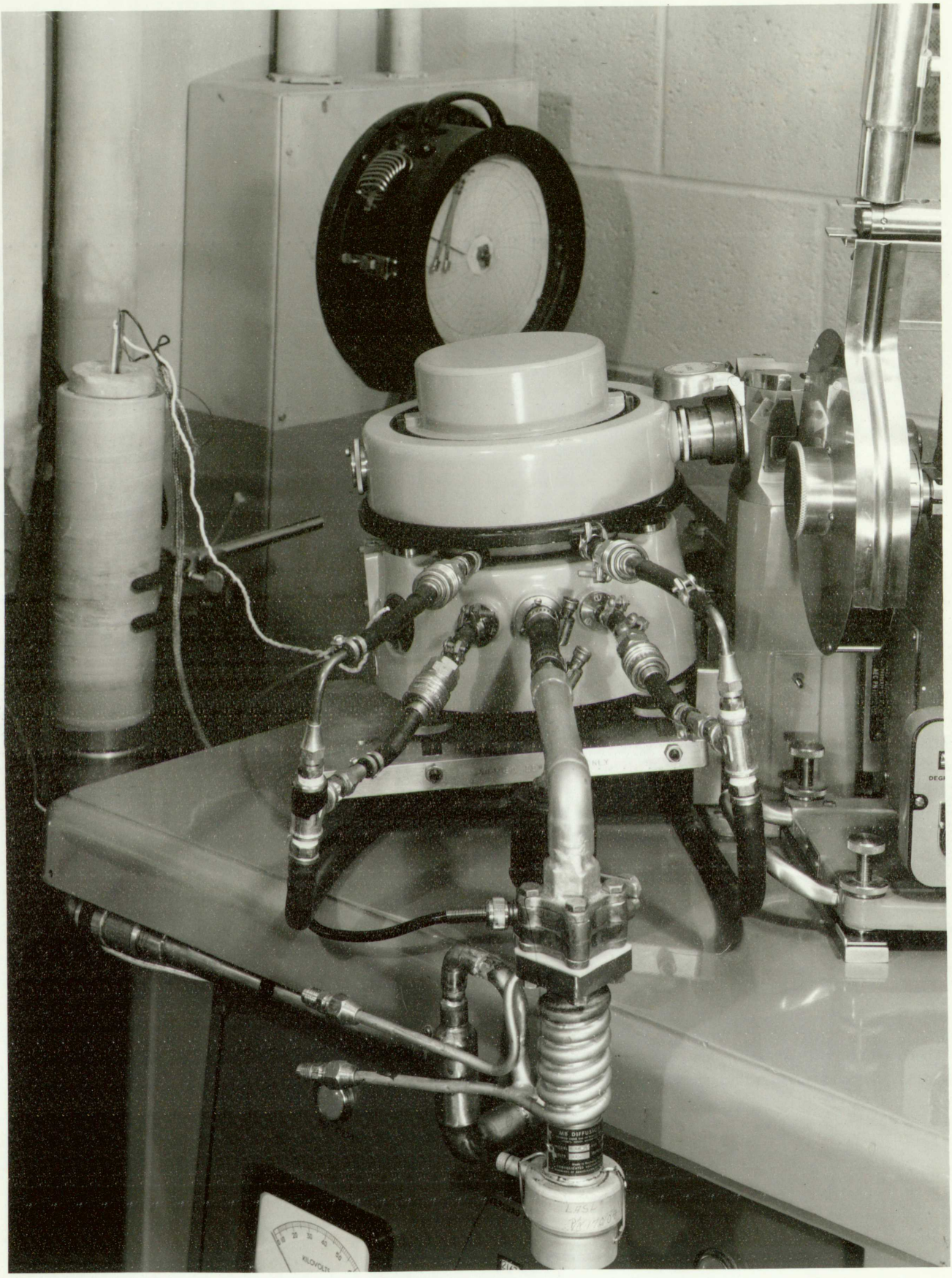

Figure 3. Unicam camera assembled and in position at the beam port (side view)

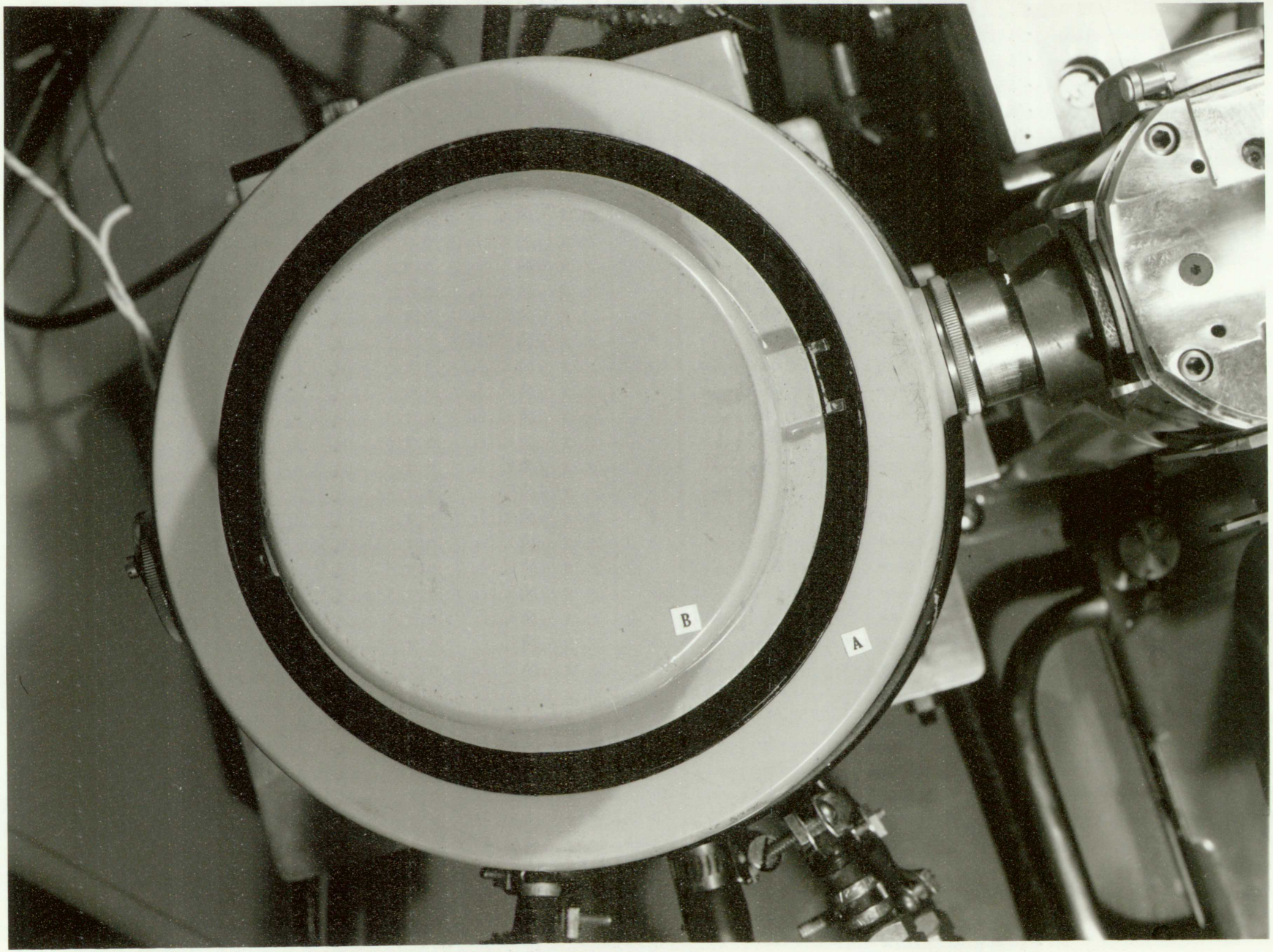

Figure 4. Unicam camera assembled and in position at the beam port (top view).

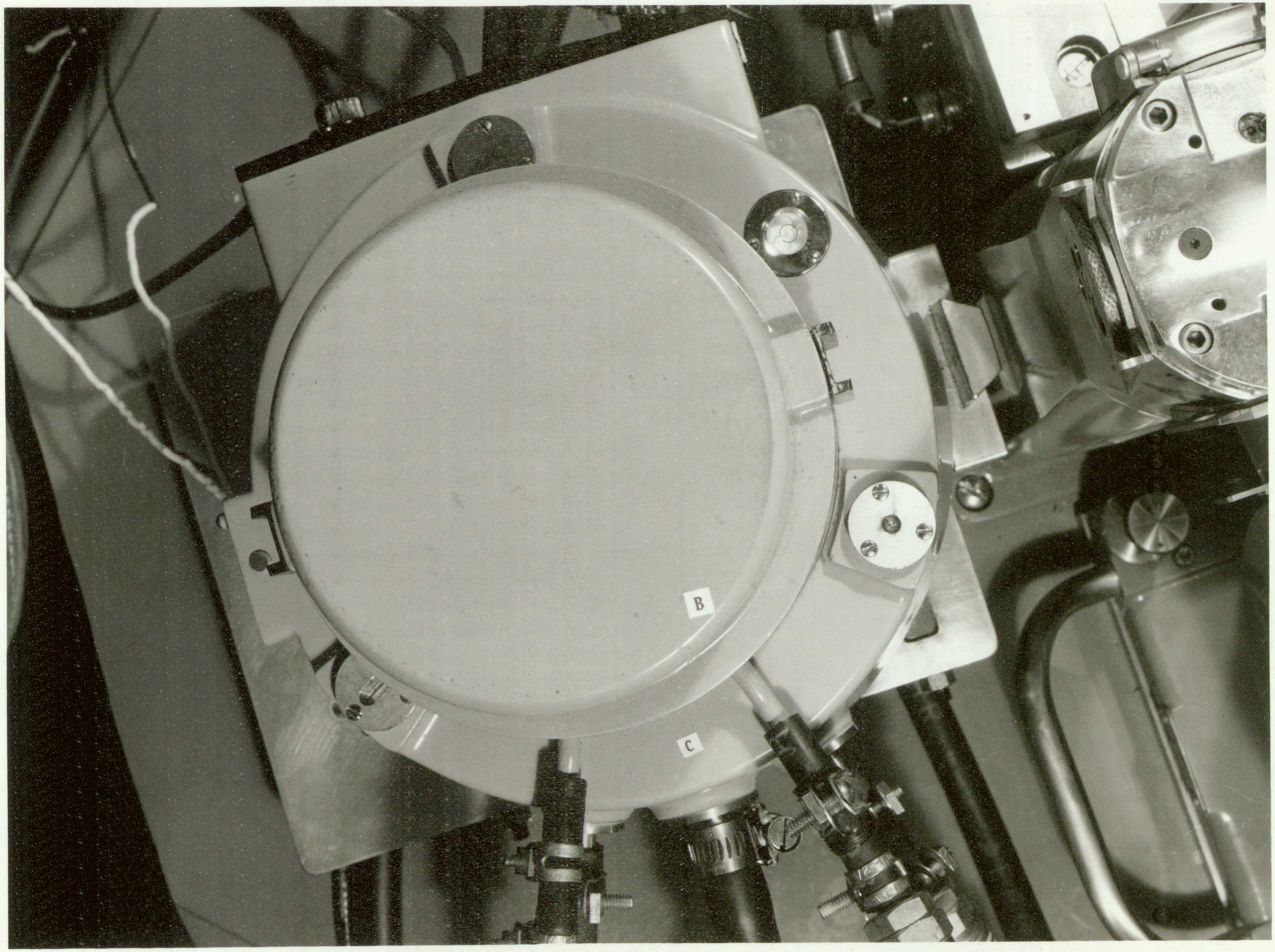

Figure 5. Unicam camera in position at the beam port with cassette removed (top view).

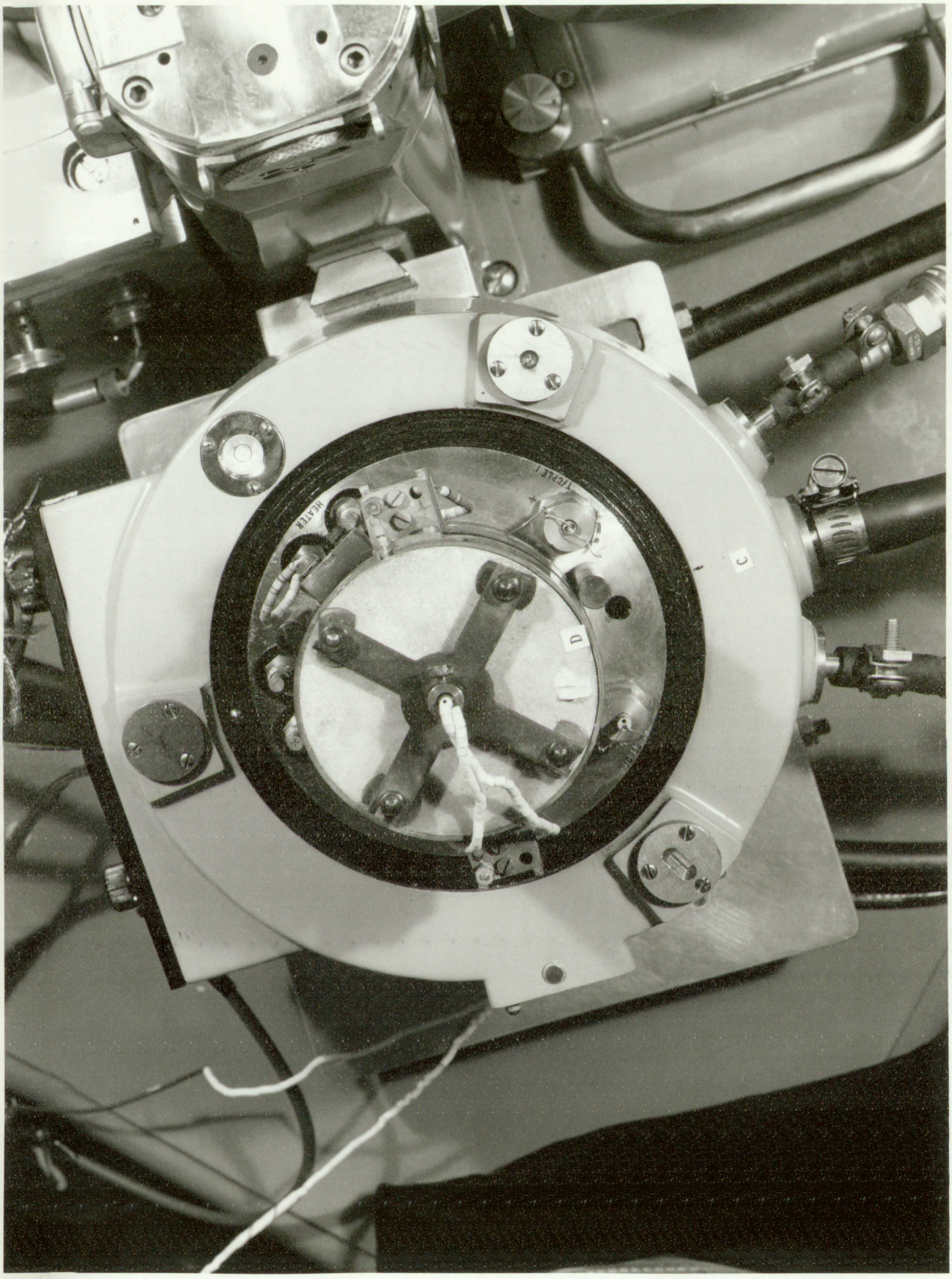

Figure 6. Unicam camera in position at the beam port with cassette and chamber removed (top view).

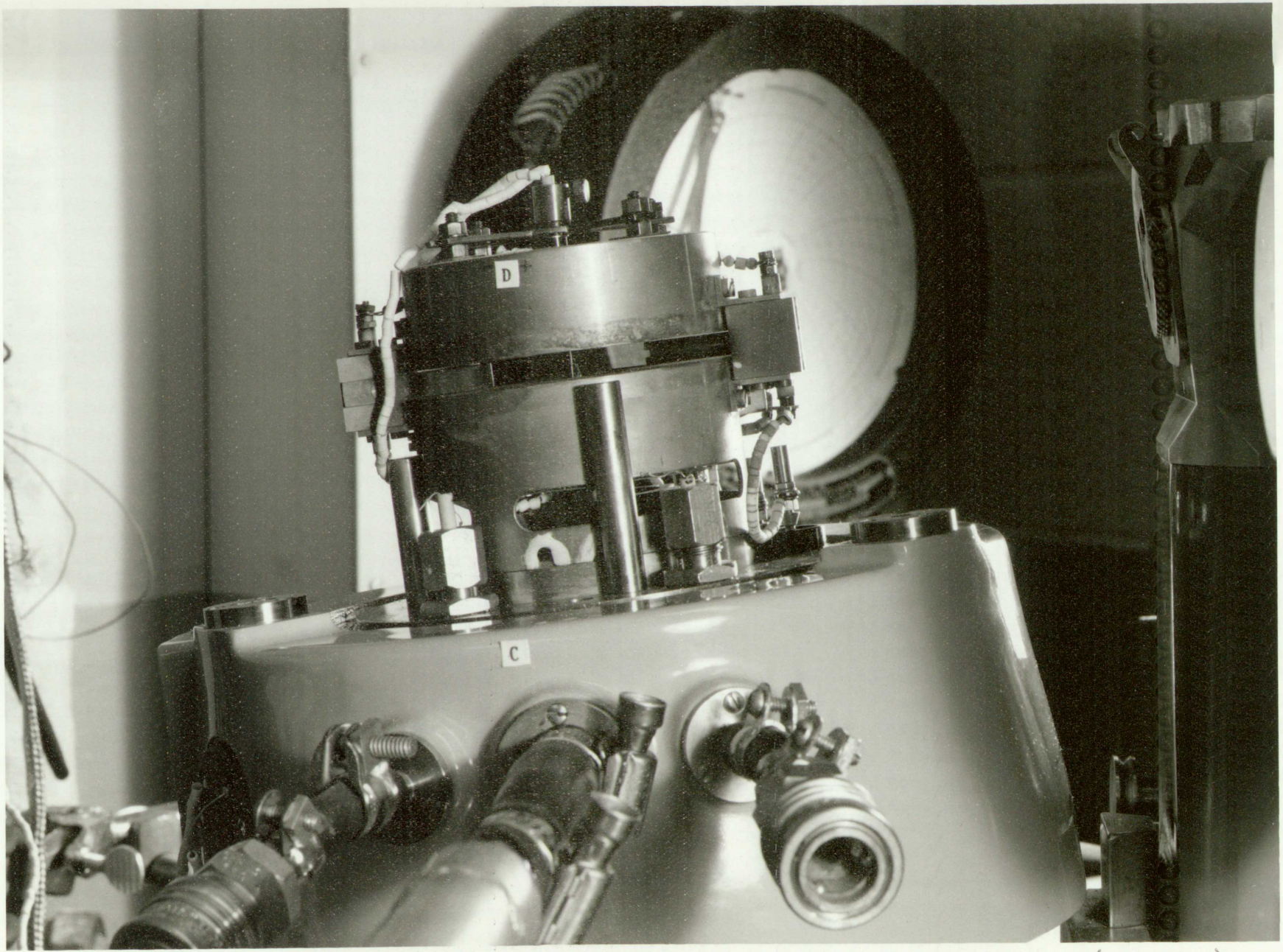

Figure 7. Unicam camera in position at the beam port with cassette and chamber removed (side view).

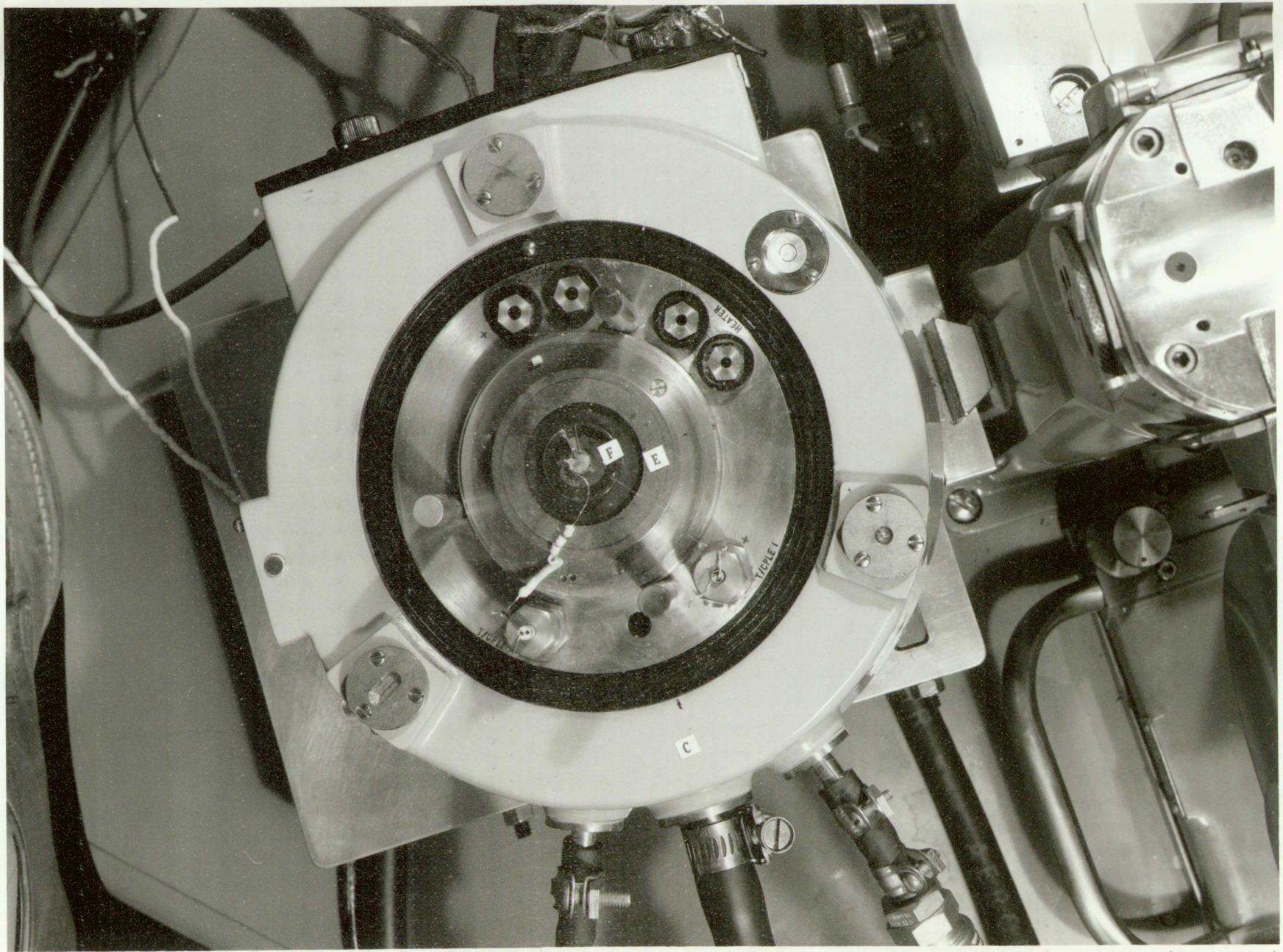

Figure 8. Unicam camera in position at the beam port with cassette, chamber, and furnace removed (top view).

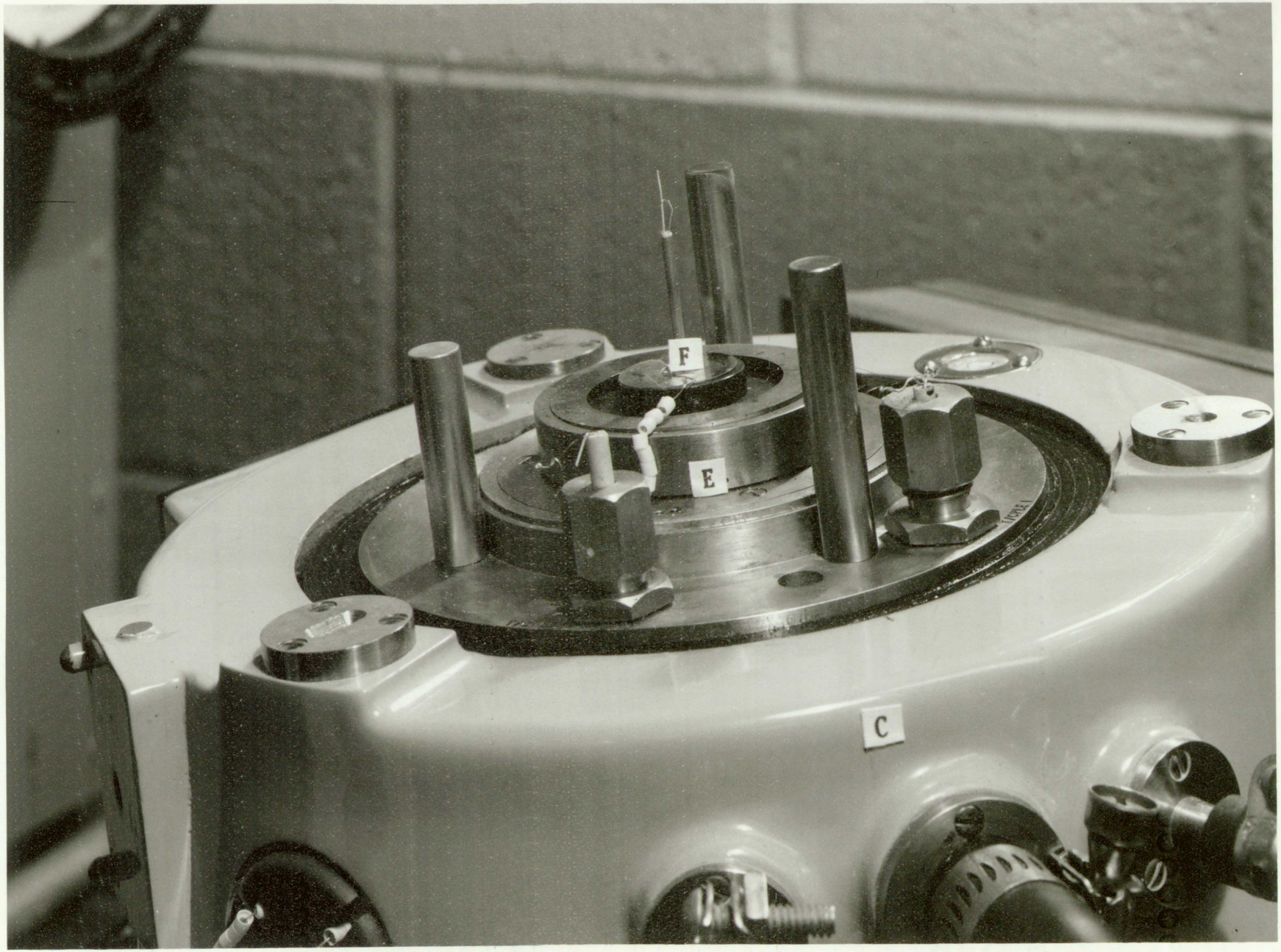

Figure 9. Unicam camera in position at the beam port with cassette, chamber, and furnace removed (side view).

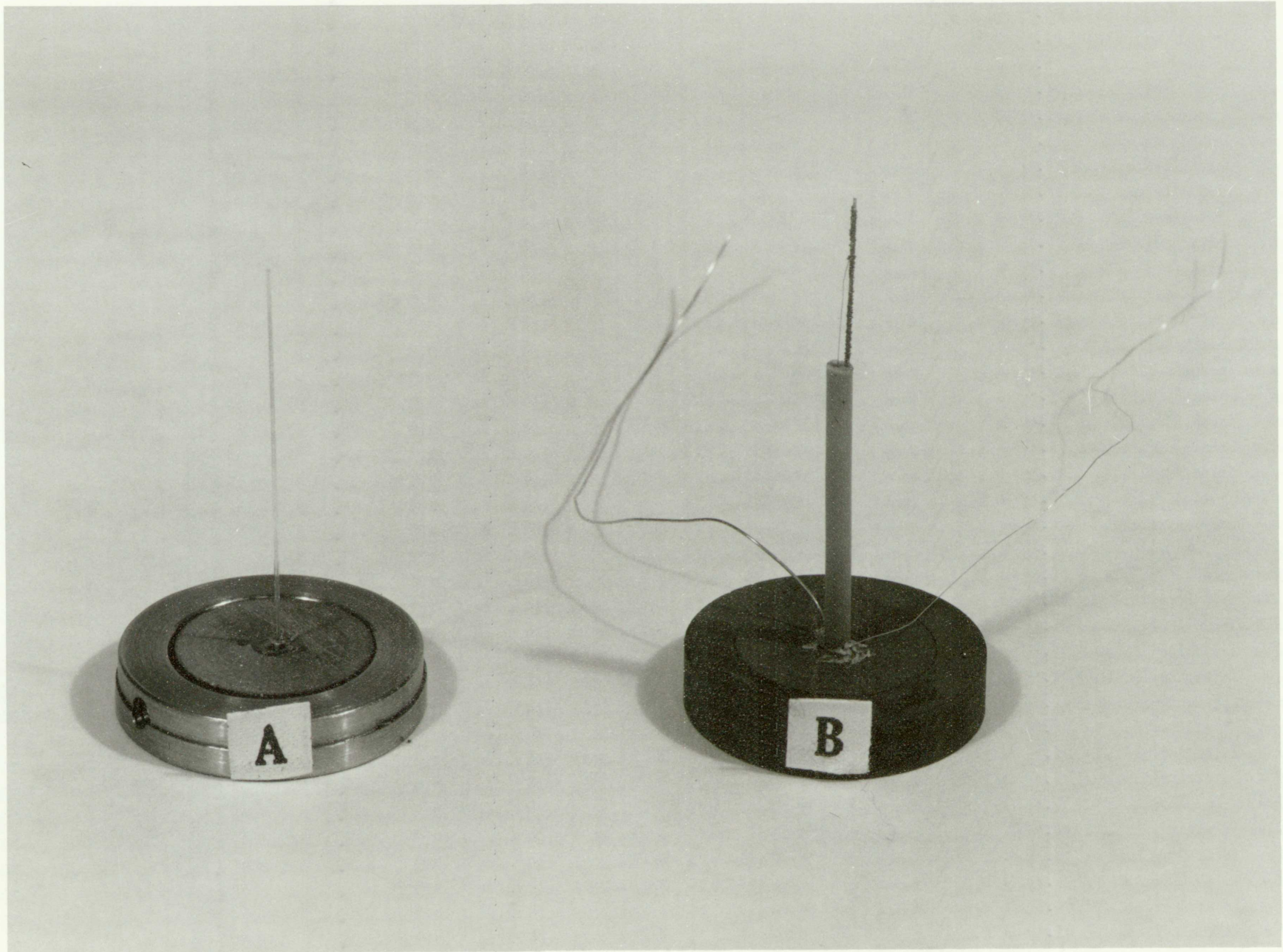

Figure 10. Typical specimens - MgO and Au powders at (A), and a Pt/Au thermocouple at (B). (Approx. 2X)

PROCEDURE

When this work was initiated, it was believed from figures obtainable in the literature that the goal of the temperature determination would have to be a measurable accuracy of 1°C or less. Most authors claimed to be within 2 or 3°C of actual specimen temperature, while a few admitted to an uncertainty of maybe 5 to 10°C. With this in mind, all of the apparatus and instrumentation was selected to satisfy the 1°C specification in the working range of 25-1000°C with the exception of possibly approaching a 2°C error as the temperature approached 1000°C.

Before any experimental work could be launched, certain aspects of the Unicam camera drew our attention. The arrangement for alignment of the sample was unsatisfactory. Some of the difficulty was found later to be in a slight misalignment of the scope furnished for this purpose. The vertical cross-hair was several degrees from true vertical, and was not aligned with the sample axis of rotation. An improved magnetic type holder was designed by the engineering section of N-1 at the Los Alamos Scientific Laboratory giving both lateral and pivotal movement of the specimen. An optical system, along with appropriate zinc sulfide screens, was made to aid in aligning the camera optics with the X-ray beam port of the source. Since only the back reflection region of the camera is utilized in precise thermal expansion work, the camera cassette was modified to receive these reflections on a single strip of film, rather than two strips, for greater precision in measuring the lattice parameters. This eliminated the cumber-

some shrinkage correction calculations and improved the precision of the lattice parameter determinations. With this simple film method, the knife edges could be removed since they were no longer needed, thus exposing more film in the high Bragg angle region. The cellophane window in the vacuum chamber is the weakest link in the vacuum system. Ordinarily, its life is short, due to embrittlement by the X-ray beam but this has been overcome by cementing thin mica over the cellophane at the beam entrance port. Thermal radiation from the furnace gap seared the cellophane window so that protective aluminum radiation shields were required. Beryllium windows have been ordered to replace the cellophane. Since the thermocouples were to be used for measurement of specimen temperature, a slip ring signal could be picked up while the specimen was rotating. This idea was finally discarded, after a long arduous battle, in favor of direct leads. It was found that contaminants created by the heat and vacuum condensed on the slip ring in a film that gave rise initially to a cyclic noise band in tune with the frequency of sample rotation, and finally serious erratic excursions on the recorder made it impossible to deduce any kind of temperature measurement. The direct lead wires, although they eventually broke from the bending by the sample rotation, usually lasted long enough for sufficient data to determine thermal expansion to 1000°C. This system of direct lead wires also necessitated replacement of the original motor drive with a reversible unit. The plug-type thermocouple connections from the vacuum chamber were replaced with glands so the thermocouple leads could be run directly to an ice bath cold junction. The connections furnished formed a cold junction of varying temperature with the Pt/Pt-10% Rh thermocouples which was inconsistent with the high precision requirements of the measuring system. This set-up was further

modified so that two thermocouples in the camera could be read simultaneously instead of the furnished mode of manually switching to either one of two provided. Ghost lines were found on initial runs with silver which were traced to leakage of the X-ray beam through the thickness of cellophane window at the entrance port of the vacuum chamber. This was corrected by imbedding lead strips in the cellophane on either side of the port to absorb the scattered rays.

To facilitate future operation of the camera furnace, the voltage applied to the furnace was calibrated against the temperature measurement from a thermocouple in the sample position. This gave a convenient reference for setting the furnace power to give the approximate temperature desired.

Constant temperature was maintained by allowing the system to come to equilibrium. The voltage of the power source was monitored with a Brown recorder to detect any voltage variations in case the temperature fluctuated during a run. Tempered circulating water controlled to $\pm$ 0.01°C was used for measurements at 25.0°C, while city (domestic) water, whose temperature did not vary more than 1°C, was used during high temperature measurements for camera cooling.

Since it was planned first to obtain measurements with a thermocouple imbedded in the sample and as near the beam path as possible without serious interference, a project of fabricating a specimen for the purpose was undertaken. Thermocouples made from wire as small as feasible to reduce conduction loss errors were to be used. These were made both beaded by flame and butt-welded electrically, the latter with a welding jig fashioned after specifications by C. M. Stover[75]. One mil and three mil diameter Pt and Pt-10% Rh

wires were used. Several designs were attempted but all proved impractical due to the fragility of both the fine thermocouple wires and the slender silica capillaries containing the sample.

In the meantime, a commercial micro thermocouple was brought to our attention by D. G. Rose and C. E. Landahl of this Laboratory. Since these were fairly rugged compared to our products, and easily obtained, they were adopted for use in the investigation of specimen temperature.

The sample was prepared as shown in Figure 11 and so positioned in the camera that the X-ray beam barely grazed the tip of the thermocouple assembly.

Beryllium was tried for a specimen holder with the intention of replacing the silica because beryllium has a much lower attenuation factor for X-radiation. Thin wall 0.010" diameter tubing was not on the market and the wall of the drilled rod that was tried was too thick, giving broad Be lines on the film. This was dropped for the time being until small sizes of beryllium tubing become economically available.

The slip ring arrangement for picking up the thermocouple signal caused extensive difficulty as mentioned earlier. It was concluded that good temperature readings could not be obtained and it was removed after about 50 runs. Direct leads were then used in conjunction with an oscillating rotation of the sample. Trouble was initially experienced with leads breaking from the bending received as a result of the oscillating motion, but this was remedied by coiling the leads adjacent to the specimen.

In order to obtain precise data for thermal expansion measurement by X-ray diffraction, it is necessary that (1) the sample be properly located in relation to the film and centered in the X-ray beam; (2) some means be provided for movement of the sample during exposure for statistical purposes in obtaining smooth lines on the film; (3) the sample be in the proper con-

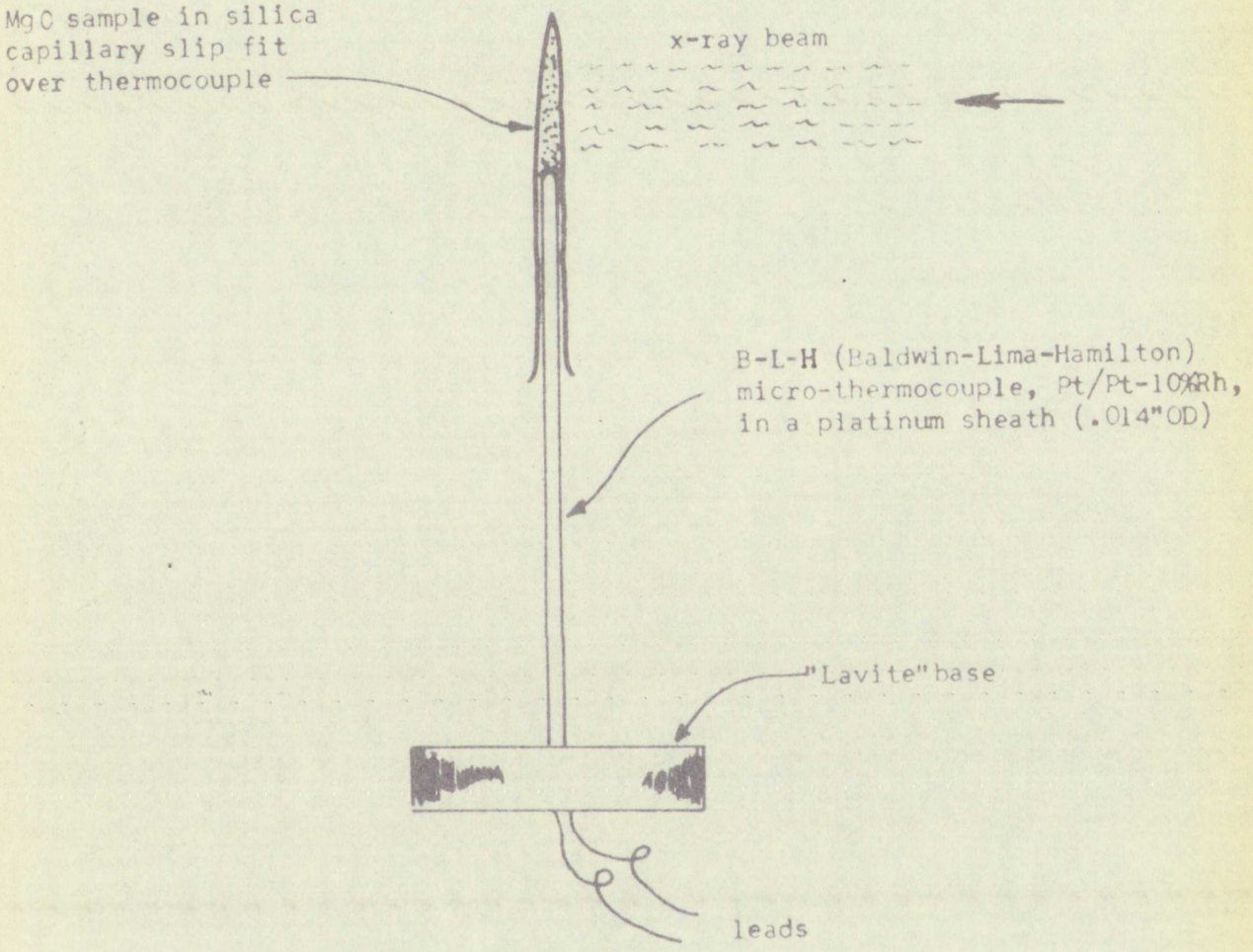

Figure 11. Sketch showing MgO specimen mounted on thermocouple.

dition, for example fine grain, free from strains and, in the case of powders, of proper particle size range; (4) precise measurement of specimen temperature be made during exposure; (5) the optics of the camera be such that clear unobstructed patterns are obtained in a reasonable length of time. All of these except (3) and (4) are taken care of in the construction and manipulation of the Unicam Camera and furnace. (4) is the main object of this investigation. However, (3) was so closely associated that it also required close attention to successfully complete the investigation.

Powdered specimens were prepared from -325 mesh sample material. The MgO was fired at 1400°C by the Bureau of Mines. The gold powder and wire were annealed by heating in vacuo to 300°C in a matter of a few minutes and slowly (about 8 hours) cooling to room temperature. The powder was placed in a sealed or unsealed silica capillary as required. This gave a specimen about .010" in diameter, and a capillary length of 38 mm was needed to allow positioning of the specimen in the beam.

The desired temperature was attained by allowing the system to come to equilibrium for any given setting of the power supply or of the tempered circulating water supply which was used for measurements at 25.0°C. The temperature of the air conditioned laboratory and the city water for cooling varied less than 1°C, giving very stable specimen temperatures at equilibrium. The range of temperatures extended from room temperature to 1000°C. Measurements were made while going up in temperature as well as coming down in order to observe any hysteresis effects in the sample. An exception was in the case of measurements of the gold lattice using the Pt-Au thermocouple; no hysteresis effects were observed on gold so to obtain quality films of the lattice parameter before grain growth interfered, exposures were made

at the high temperatures in as short a time as possible and the temperature then decreased for the exposures at lower temperatures.

Films were developed for 5 to 7 minutes depending on temperature, washed for 30 seconds, fixed for 15 minutes, and washed for 30 minutes. Ilford "Industrial G" X-ray film was used in all tests to reduce required exposure time.

The time for exposure depended somewhat on sample temperature, being longer at elevated temperature. Exposure time for MgO was 8-10 hours; for the MgO + Au mixture, it was 10-12 hours; for Au, it was 4-7 hours.

Films were measured on a viewer which could be read to the nearest .005 cm. Each film was read by three persons. All lattice parameters and their standard deviations were determined on an IBM 704 computer by the method of Vogel and Kempter[76] discussed under Calculations. Briefly, the systematic errors such as film shrinkage and specimen eccentricity are accounted for by the code which is based on Bragg's law, θ

$$\lambda = 2 d_{hkl} \sin \theta_{hkl}$$

where: λ = wavelength of the radiation, A°

d = interplanar spacing, A°

θ = Bragg angle

h,k,l = Miller indices

θ is measured indirectly on the viewer; the segment of film circumference intercepted is determined from the viewer measurement and knowing the camera diameter this is translated into values of θ. λ is known from the characteristic wavelengths of the target, and the $\underline{d}$ spacing can be calculated from the above equation. The lattice parameter is obtained by extrapolating the curve of $\underline{a}$ versus $\phi \tan \phi$ (where $\phi = 90^{\circ} - \theta$) to $\phi = 0$, with each point being statistically weighted. A more detailed account of the method is

given under Calculations. It can be seen from this that the more points produced, as in any curve, and the nearer the values of ϕ approach zero (i.e., $\theta = 90^{\circ}$), the more precise final values of $\underline{a}$ will be.

Several runs were always made in the region of room temperature to obtain a feel for the sensitivity of the sample materials to our measurements of $\underline{a}$ versus temperature in answer to the question "what is the minimum temperature change in which the lattice movement can be observed by viewing the respective films?" This was about 2° in the case of gold and 5° for MgO.

In a typical test, say of MgO, with an internal standard of Au which has been calibrated using the Pt/Au thermocouple specimen described under Apparatus, the sample mixture is prepared as described above and mounted inside the camera furnace and vacuum chamber. The film cassette with Ilford "Industrial G" film is placed in position. After the temperature of the furnace has come to equilibrium, as indicated by the furnace thermocouple, at say about $500^{\circ}C$, the X-ray beam is turned on. After 10 hours exposure, the film is removed, developed, and dried. The lattice patterns obtained on the film are then measured on the viewer by three persons to obtain good statistics. These values, along with the camera diameter and the wavelengths of the X-ray radiation, are submitted to the IBM 704 computer for translation into values of the lattice parameter of MgO and Au. The temperature is obtained by reference to the lattice parameter versus temperature for Au in the Appendix.

CALCULATIONS

1.

Temperature Difference Between Sample and Thermocouple

The orientation of the sample and thermocouple in the furnace is shown in Figure 12. The top of the sample is "looking at" the cold opening in the top of the furnace. In order to simplify calculations, the furnace was considered to be a spherical enclosure with no gap. No data on the thermal conductivity of MgO powder was found, so it was assumed that the properties of silica would show similar temperature variations since the MgO sample is enclosed in a silica capillary.

Referring to the mathematical model of the sample and thermocouple lying along the x-axis in Figure 13, the heat balance for a dx section is that,

Heat loss by conduction = heat gain by radiation

or $$-\frac{d}{dx}\left(k A \frac{dT}{dx}\right) dx = (C\,dx)\,\sigma\,\epsilon\,(T_f^4 - T^4)$$

where k = thermal conductivity

A = cross-section area at x

T = temperature at x

C = circumference at x

σ = Stefan-Boltzmann constant

ϵ = emissivity

T_f = furnace temperature

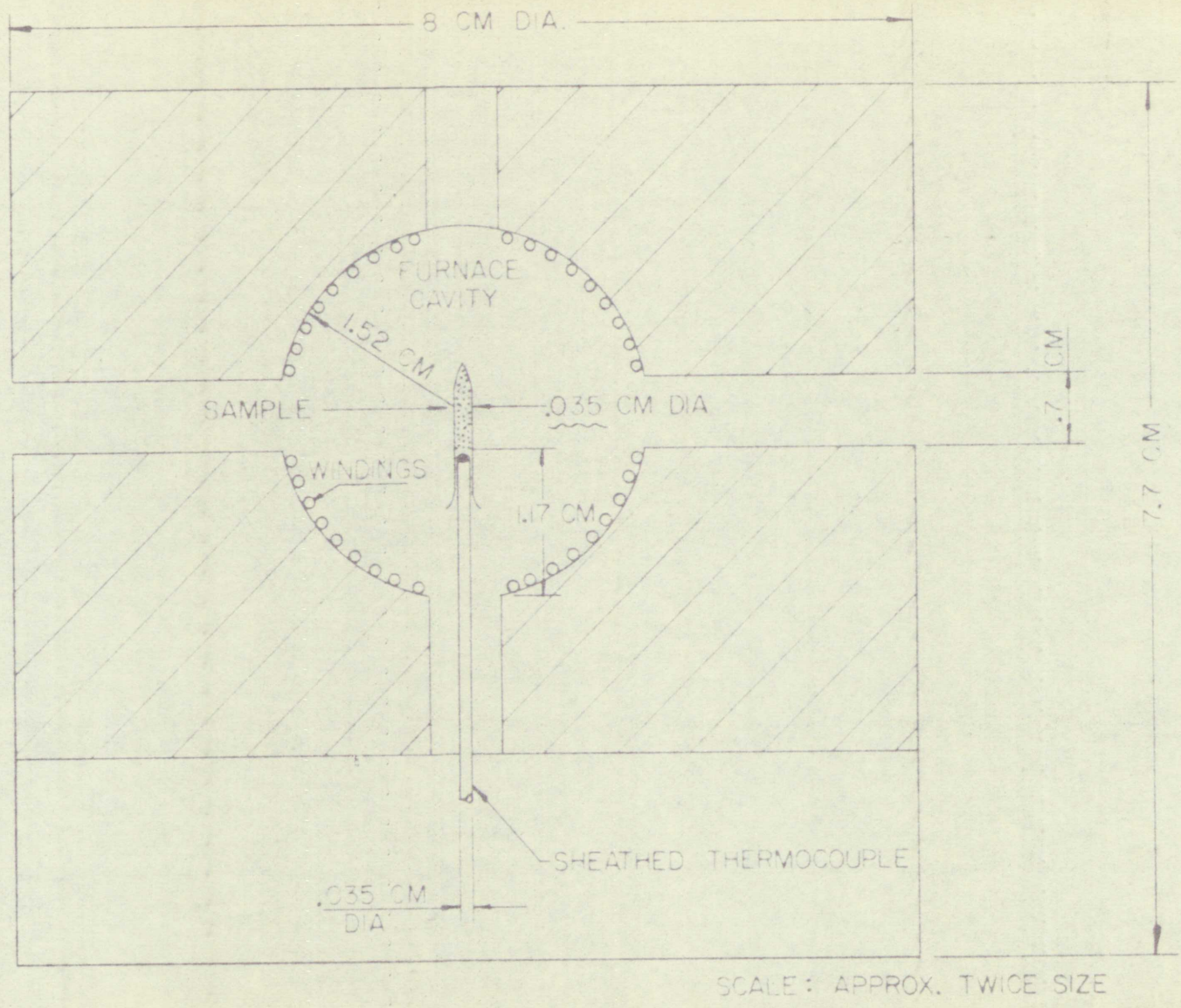

Figure 12. Sketch showing the arrangement and location of the MgO specimen and thermocouple in the furnace.

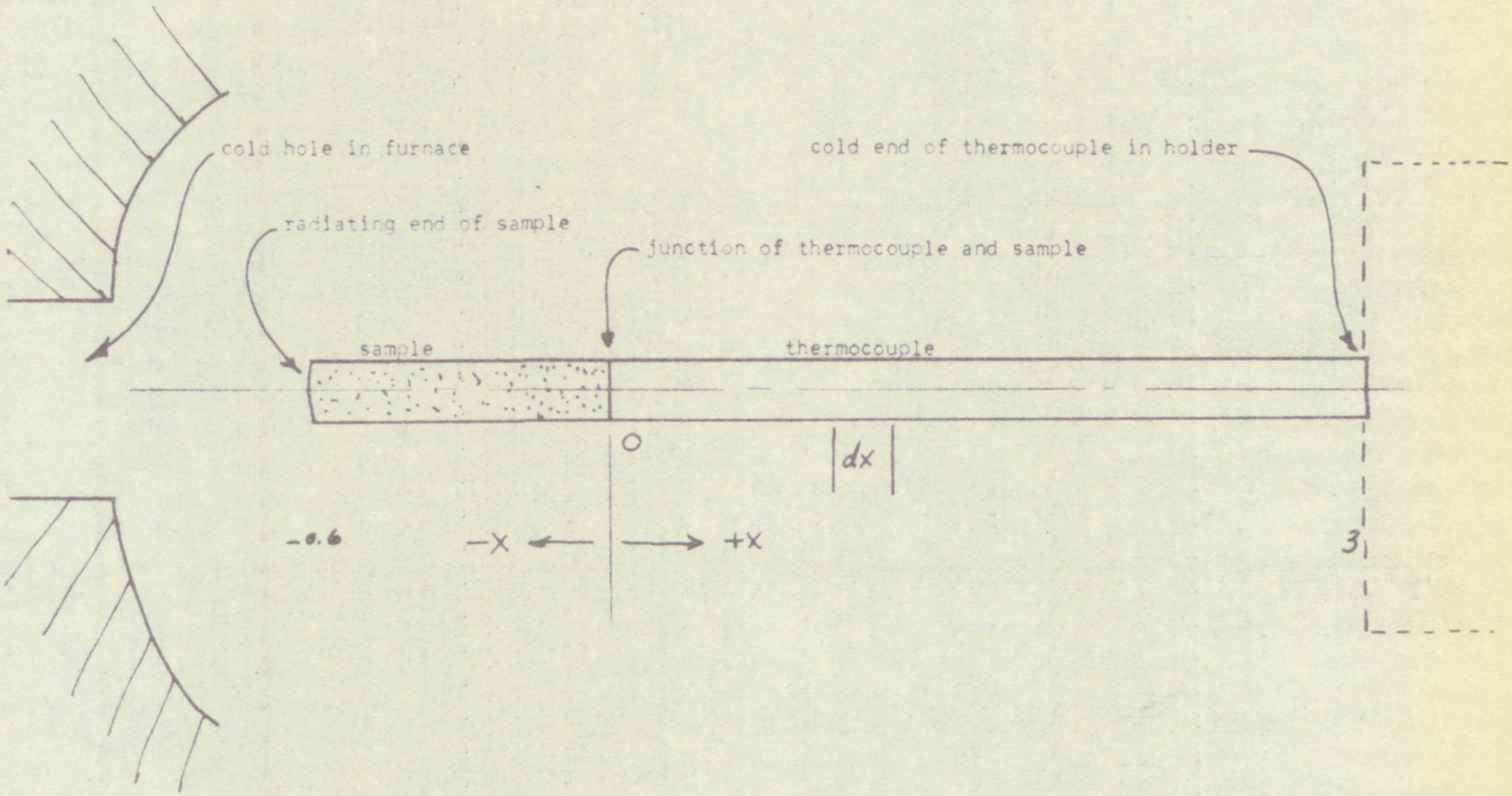

Figure 13. Mathematical model of sample and thermocouple for heat transfer calculation.

This simplifies to

$$\frac{d^2T}{dx^2} = \frac{C\sigma\epsilon}{kA}(T^4 - T_f^4)$$

If we let $\tau = 1 - \frac{T}{T_f}$, $\frac{d^2T}{dx^2} = -T_f \frac{d^2\tau}{dx^2}$, and $\frac{T}{T_f} = 1 - \tau$

Substituting,

$$-T_f \frac{d^2\tau}{dx^2} = \frac{C\sigma\epsilon}{kA} T_f^4 [(1-\tau)^4 - 1]$$

Expanding $(1-\tau)^4$ by the Taylor's series and dropping powers of τ since they are small,

$$(1-\tau)^4 \simeq 1 - 4\tau$$

Then

$$-\frac{d^2\tau}{dx^2} = \frac{C\sigma\epsilon}{kA} T_f^3 [(1 - 4\tau - 1)] = -\frac{4C\sigma\epsilon}{kA} T_f^3 \tau$$

Let $\lambda = \sqrt{\frac{4C\sigma\epsilon}{kA} T_f^3}\, x$, and then $dx^2 = \frac{d\lambda^2}{\frac{4C\sigma\epsilon}{kA} T_f^3}$

Substituting,

$$\frac{d^2\tau}{d\lambda^2} = \tau$$

The general solution of this equation is,

$$\tau = D e^{\lambda} + E e^{-\lambda} \qquad (1)$$

At the radiating end below the cold hole in the top of the furnace, using a heat balance as above,

$$kA \frac{dT}{dx} = \frac{A\sigma\epsilon}{k} T^4 - \frac{A\sigma\epsilon}{k} f T_f^4$$

where f is the shape factor for the furnace seen by the end.

Using the same substitutions as above for Equation (1), the following is obtained for the radiating end,

$$4\tau - \alpha \frac{d\tau}{d\lambda} = 1 - f \quad \text{where } \alpha^2 = \frac{4\,Ck}{A\sigma\epsilon T_f^3} \tag{2}$$

For the sample ($x < 0$) from Equation (1),

$$\tau = D_s e^{r\lambda_s} + E_s e^{-r\lambda_s} \tag{3}$$

where λ_s = the value of λ in the sample ($x < 0$), and r is the ratio of thermal conductivities relating λ for the sample to λ for the thermocouple.

For the thermocouple ($x > 0$) from Equation (1),

$$\tau = D_t e^{\lambda_t} + E_t e^{-\lambda_t} \tag{4}$$

where λ_t = the value of λ in the thermocouple ($x > 0$).

At the junction ($x = 0$),

$$k_s A \left.\frac{dT}{dx}\right|_{x = 0-} = k_t A \left.\frac{dT}{dx}\right|_{x = 0+} \tag{5}$$

Boundary conditions for determining the constants D_t, E_t, D_s and E_s:

a) At the holder on the cold end of the thermocouple from Equation (1)

$$\tau_h = D_t e^{\lambda_t} + E_t e^{-\lambda_t} \tag{6}$$

b) At the radiating end from Equation (2)

$$D_s e^{r\lambda_e} (4 - \alpha) + E_s e^{-r\lambda_e} (4 + \alpha) = 1 - f \tag{7}$$

c) At the junction (x = 0) from Equation (1)

$$\tau = D_t + E_t = D_s + E_s \tag{8}$$

$$\therefore D_t + E_t - D_s - E_s = 0$$

d) On either side of x = 0 from Equation (5)

$$\left.\frac{d\tau}{d\lambda}\right|_{x = 0-} = \frac{k_t}{k_s} \left.\frac{d\tau}{d\lambda}\right|_{x = 0+} \qquad \left(\frac{k_t}{k_s} = r^2\right)$$

and with the values of $\frac{d\tau}{d\lambda}$ from equations (3) and (4),

$$rD_s - rE_s = r^2 (D_t - E_t) \tag{9}$$

Since the main interest is in the temperature difference of the sample, and thermocouple tip at x = 0, the following relation is derived from Equation (1),

$$\tau_s - \tau_t = D_s e^{r\lambda_s} + E_s e^{-r\lambda_s} - D_s - E_s \tag{10}$$

and,

$$\Delta T = T_f - T_s = T_f (\tau_s - \tau_f) \tag{11}$$

To solve for ΔT, the values of the constants D_s and E_s can be found from the determinant of the coefficients of Equations (6), (7), (8), and (9).

$\frac{D_t}{e^{\lambda_h}}$	$\frac{E_t}{e^{-\lambda_h}}$	$\frac{D_s}{0}$	$\frac{E_s}{0}$	τ_h
0	0	$(4-\alpha) e^{r\lambda_e}$	$(4+\alpha) e^{-r\lambda_e} = 1$	$- f$
1	1	-1	-1	0
-r	r	1	-1	0

Letting Δ = determinant of coefficients of D_t, E_t, D_s and E_s,

$$\Delta = e^{\lambda_h} \left\{ [2e^{r\lambda_e} (4-\alpha)] + (1 + r) [-e^{r\lambda_e} (4-\alpha) + e^{-r\lambda_e} (4 + \alpha)] \right\}$$

$$+ e^{-\lambda_h} \left\{ [2e^{r\lambda_e} (4-\alpha) - (1-r) [-e^{r\lambda_e} (4-\alpha) + e^{-r\lambda_e} (4+\alpha)] \right\} \qquad (12)$$

Let $\Delta (E_s)$ denote the determinant Δ with the E_s column replaced by the column of coefficients on the right of the equation. Evaluate obtaining,

$$\Delta (E_s) = (1 - f) [e^{\lambda_h} (1 + r) - e^{-\lambda_h} (1 - r)] - \tau_h [e^{r\lambda_e} (4 - \alpha) 2r] \qquad (13)$$

By the same procedure, $\Delta (D_s)$ is obtained,

$$\Delta (D_s) = 2 \tau_h re^{-r\lambda_e} (4+\alpha) - (1 - f) [e^{\lambda_h} (r - 1) + e^{-\lambda_h} (r + 1)] \qquad (14)$$

The constants D_s and E_s for Equation (10) are then calculated from the relations,

$$E_s = \frac{\Delta (E_s)}{\Delta} \qquad (15)$$

$$D_s = \frac{\Delta (D_s)}{\Delta} \qquad (16)$$

ΔT at a furnace temperature of $700^{\circ}K$ was calculated as follows using properties and constants from references (77), (78), and (79).

$C = 0.113$ cm

$A = 0.0008$ cm^2

$\sigma = 1.36 \times 10^{-12}$ cal/cm^2 $^\circ$K^4 sec

$f = 0.2$

ϵ = assumed equal to 1 for an enclosure

k (platinum) $= 0.19$ cal/cm sec$^\circ$K

k (silica) $= 0.0033$ cal/cm sec$^\circ$K

$$r = \sqrt{\frac{k\,(pt)}{k\,(Si)}} = \sqrt{\frac{0.19}{0.0033}} = 7.6$$

Calculating the values of λ and α:

$$\lambda_h \text{ (for Pt at sample holder, } x = 3.\text{ cm)} = 3. \sqrt{\frac{4\,(.113)(1.36 \times 10^{-12})}{(.19)\,(.0008)}\,(700)^3}$$

$$= 3.5$$

$$\lambda_e = \lambda_s \text{ (for Pt at radiating end, } x = -0.6 \text{ cm)}$$

$$= (-0.6) \sqrt{\frac{4\,(.113)(1.36 \times 10^{-12})}{(.19)(.0008)}\,(700)^3} = -0.7$$

$$\alpha \text{ (for Pt)} = \sqrt{\frac{4\,(.113)(.19)}{(.0008)(1.36 \times 10^{-12})(700)^3}} = 64.$$

Assuming the temperature of the water cooled holder to be near room temperature, say 300°K,

then $$\tau_h = 1 - \frac{300}{700} = 0.57$$

Substituting the values of λ, α, and r in Equations (12), (13), and (14), and using the relations in (15) and (16),

$$E_s = 5.95 \times 10^{-5}$$

$$D_s = 0.03$$

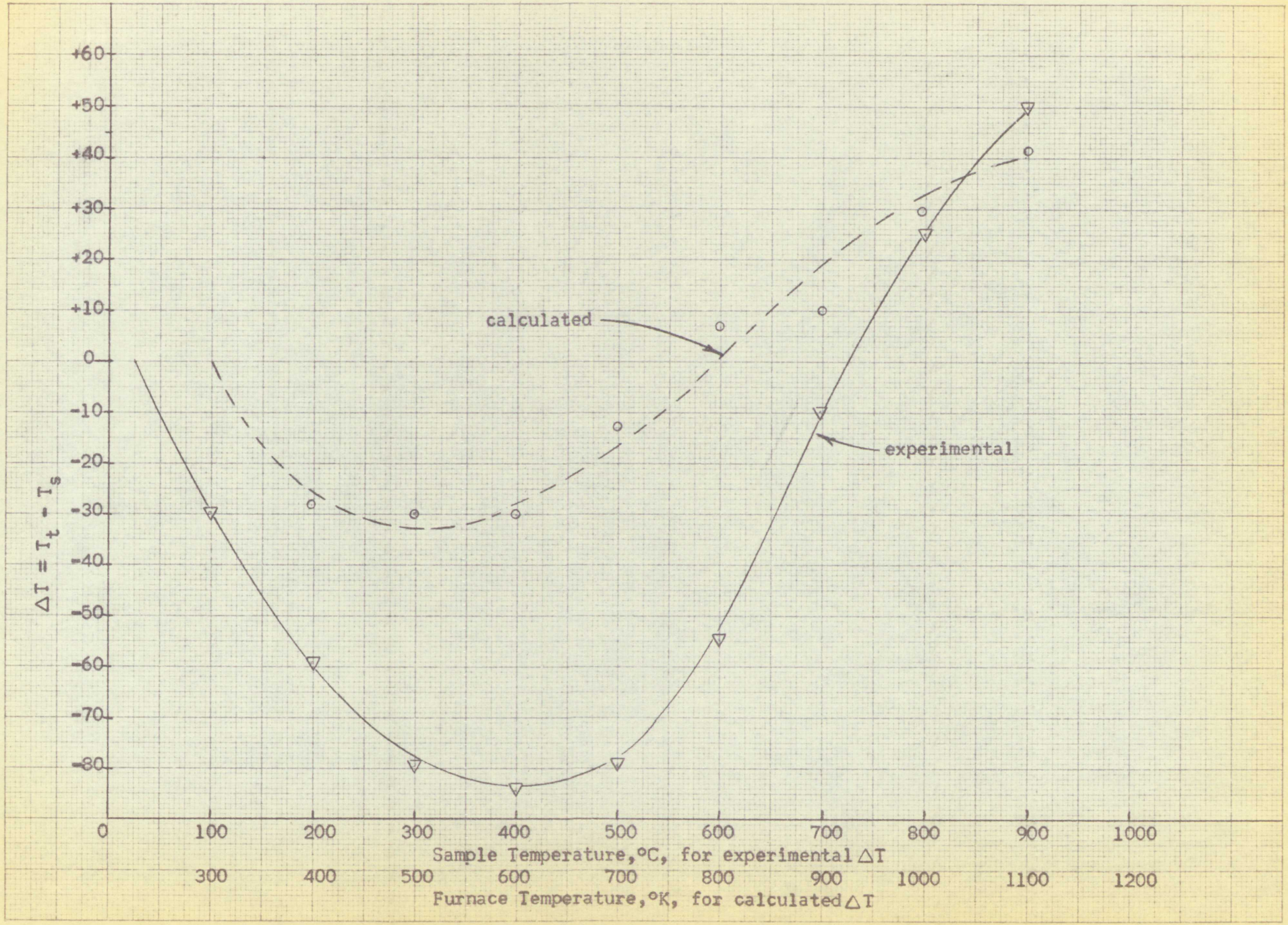

Figure 14. Comparison between experimental and calculated values of $T_t - T_s$.

From Equations (10) and (11),

$$\tau_s - \tau_t = (0.03)(0.005) + (5.95 \times 10^{-5} \times 200.) - (0.03) - (5.95 \times 10^{-5})$$

$$= - 0.018$$

$$\Delta T = 700 (- 0.018) = -12.6^{\circ}K \text{ or } ^{\circ}C$$

which means that the thermocouple is 12.6° cooler than the sample when the furnace is at 700°C. Values of ΔT were similarly calculated for other temperatures to give the "calculated" curve in Figure 14.

For comparison, corresponding ΔT's were found for the "experimental" curve by measuring in Figure 19 the difference between the "thermocouple" and "Au standard" curves at any given lattice parameter and taking the value of the temperature for the Au standard to be the true sample temperature. For example, at a temperature of 400°C the Au standard method indicates that the thermocouple is about 80°C colder than the sample.

2.

Measurement of Lattice Parameters by the Vogel and Kempter Method

All calculations of lattice parameters were performed on an IBM 704 computer using the method of Vogel and Kempter[76]. A graphical illustration of the IBM 704 method as used in the calculation of the room temperature lattice parameter of gold is shown below.

The diffraction pattern is produced on the film as shown in principle in Figure 15, illustrating how the diffraction cones from the sample intercept the film producing a pattern similar to the sketch in Figure 16 for Au at 25°C. The raw data for an actual run of gold at 25°C was as follows:

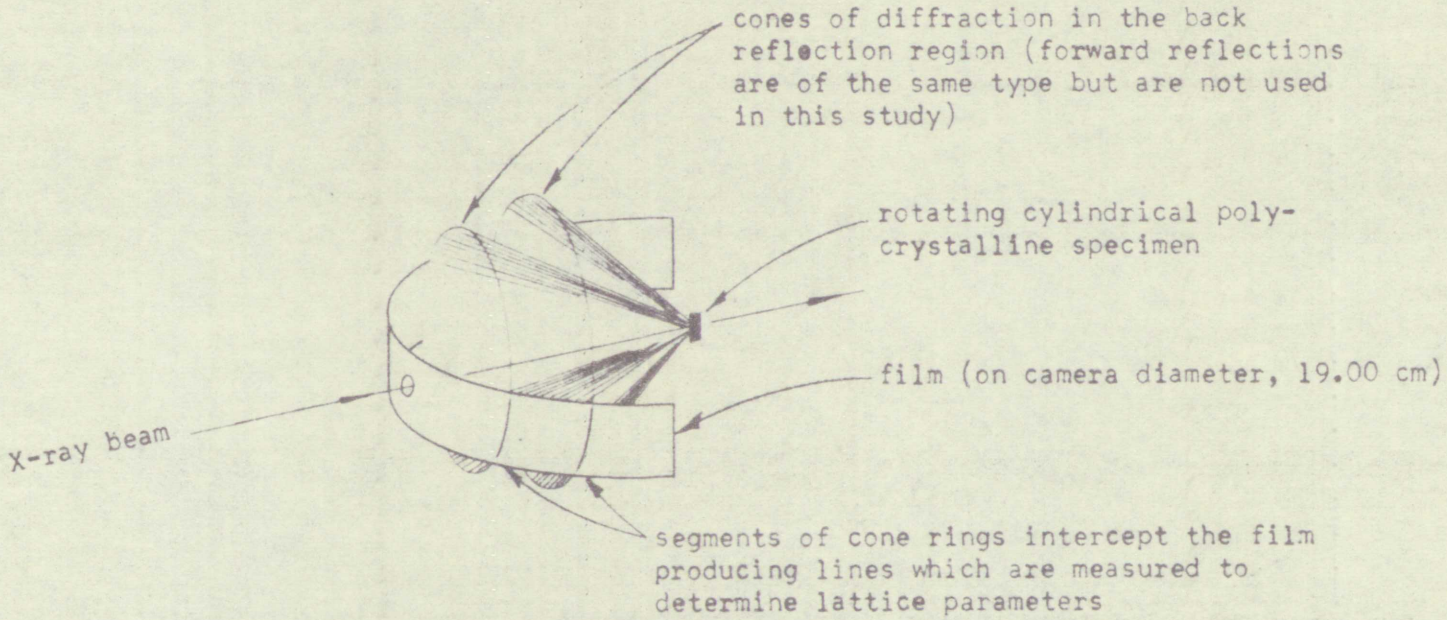

Figure 15. Sketch showing the relation of film to sample and diffracted beam in the Debye - Scherrer camera.

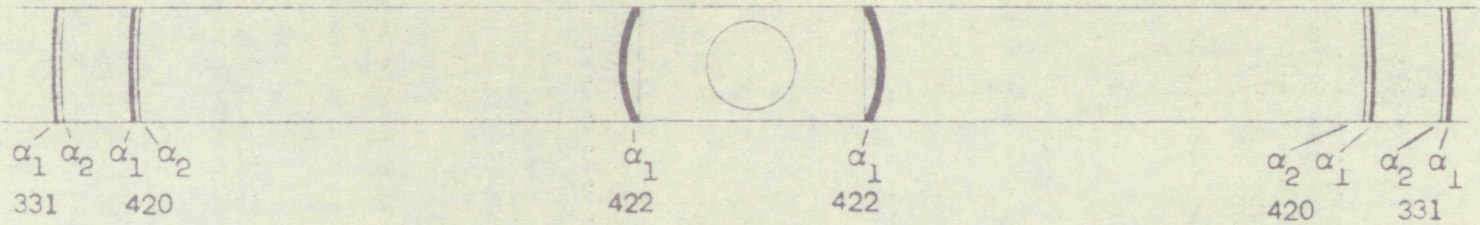

Figure 16. Sketch of film obtained for gold at room temperature showing the 331, 420, and 422 lines used in the sample calculations.

h	k	l	Kα	S, cm.
3	3	1	1	18.380
3	3	1	2	18.218
4	2	0	1	16.390
4	2	0	2	16.200
4	2	2	1	3.550

where h, k, and l are the Miller indices designating the particular diffraction lines.

Kα indicates the line produced from λ_1 or λ_2 wavelengths (NiKα radiation was used for all X-ray diffraction studies in this thesis)

S = ring diameter (in cm.) as measured on film.

The raw data for the 331 $K\alpha_1$ line will be used for the sample calculations and the calculated values for all lines obtained in the same manner are tabulated below:

$\frac{S}{D} = \Phi$ (radians) for the Debye-Scherrer camera

where

D = diameter of the Debye-Scherrer camera, 19.00 cm

$\frac{\Phi}{2} = \phi = \frac{\pi}{2} - \theta$

where

θ is the Bragg angle in the Bragg equation $\lambda = 2\, d_{hkl} \sin \theta_{hkl}$

where

λ = the X-ray wavelength in Angstrom units

d = the interplanar spacing in Angstrom units

then

$\underline{a}$, the lattice parameter = $d_{hkl} \sqrt{h^2 + k^2 + l^2}$

(uncorrected for systematic errors)

For the 331 $K\alpha_1$ line,

$$\Phi = \frac{18.380}{19.00} = .\underline{9674} \text{ radians}$$

$$\phi = \frac{\Phi}{2} = .\underline{4837} \text{ radians}$$

$$\theta = \frac{\pi}{2} - \phi = 1.5708 - .4837 = 1.0871 \text{ radians}$$

$\sin \theta = .\underline{8852}$

λ for $NiK\alpha_1$ radiation = 1.65784 A°

$$d = \frac{\lambda}{2 \sin \theta} = \frac{1.65784}{2(.8852)} = .\underline{93642} \text{ A}^{\circ}$$

and

$$a = d \sqrt{h^2 + k^2 + l^2} = .9364 \sqrt{3^2 + 3^2 + 1^2} = .9364 \times 4.3589 = \underline{4.08176 \text{ A}^{\circ}}$$

Tabulation of values for all lines.

h	k	l	K α	Φ, radians	ϕ, radians	sin θ	d_{hkl}, A°	a_{hkl}, A°
3	3	1	1	.9674	.4837	.8852	.93642	4.08176
3	3	1	2	.9588	.4794	.8873	.93636	4.08150
4	2	0	1	.8626	.4313	.9084	.91250	4.08082
4	2	0	2	.8526	.4263	.9107	.91230	4.07993
4	2	2	1	.1868	.0934	.9957	.83249	4.07835

The systematic errors in $\Delta a_o / a_o$ (where $\underline{a}_o$ is the "true" lattice parameter) are directly proportional to $\phi \tan \phi$ in the back reflection region, and approach zero as θ approaches $\frac{\pi}{2}$ radians [80], i.e. $\phi \tan \phi$ approaches zero. Therefore, by plotting $\underline{a}$ versus $\phi \tan \phi$ and extrapolating to $\phi \tan \phi = 0$, a precise value of $\underline{a}_o$ is obtained.

Calculating $\phi \tan \phi$ for the 311 $K\alpha_1$ line:

ϕ from above calculation is .4837 radians, then $\tan \phi = .5255$ and,

$\phi \tan \phi = .4837 \times .5255 = .254$ radians.

Tabulation of values for all lines,

h	k	l	K α	$\phi \tan \phi$, radians
3	3	1	1	.254
3	3	1	2	.249
4	2	0	1	.198
4	2	0	2	.193
4	2	2	1	.009

Plotting a versus $\phi \tan \phi$ in Figure 17, and extrapolating to $\phi \tan \phi = 0$, the "true" lattice parameter (a_o) of 4.0782 Å is obtained. A more precise value of 4.07852 ± 0.00006 Å was obtained for this run on the IBM 704 computer using the method of Vogel and Kempter[76]. However, S values by three readers (in order to obtain better statistics) were used in the calculation, and in addition the method gives a statistical weight (approximately equal to $\csc^2 2\phi$) to every point. This weighting is most important since the weighting factor approaches infinity as ϕ approaches zero (i.e., θ approaches 90°). It was for this reason that a nickel target-which gives a very high Bragg angle 422 line for the gold standard-was chosen. The systematic errors[80] considered are:

1) Camera radius error
2) Film shrinkage
3) Specimen eccentricity
4) Specimen absorption
5) Horizontal beam divergence
6) Vertical beam divergence

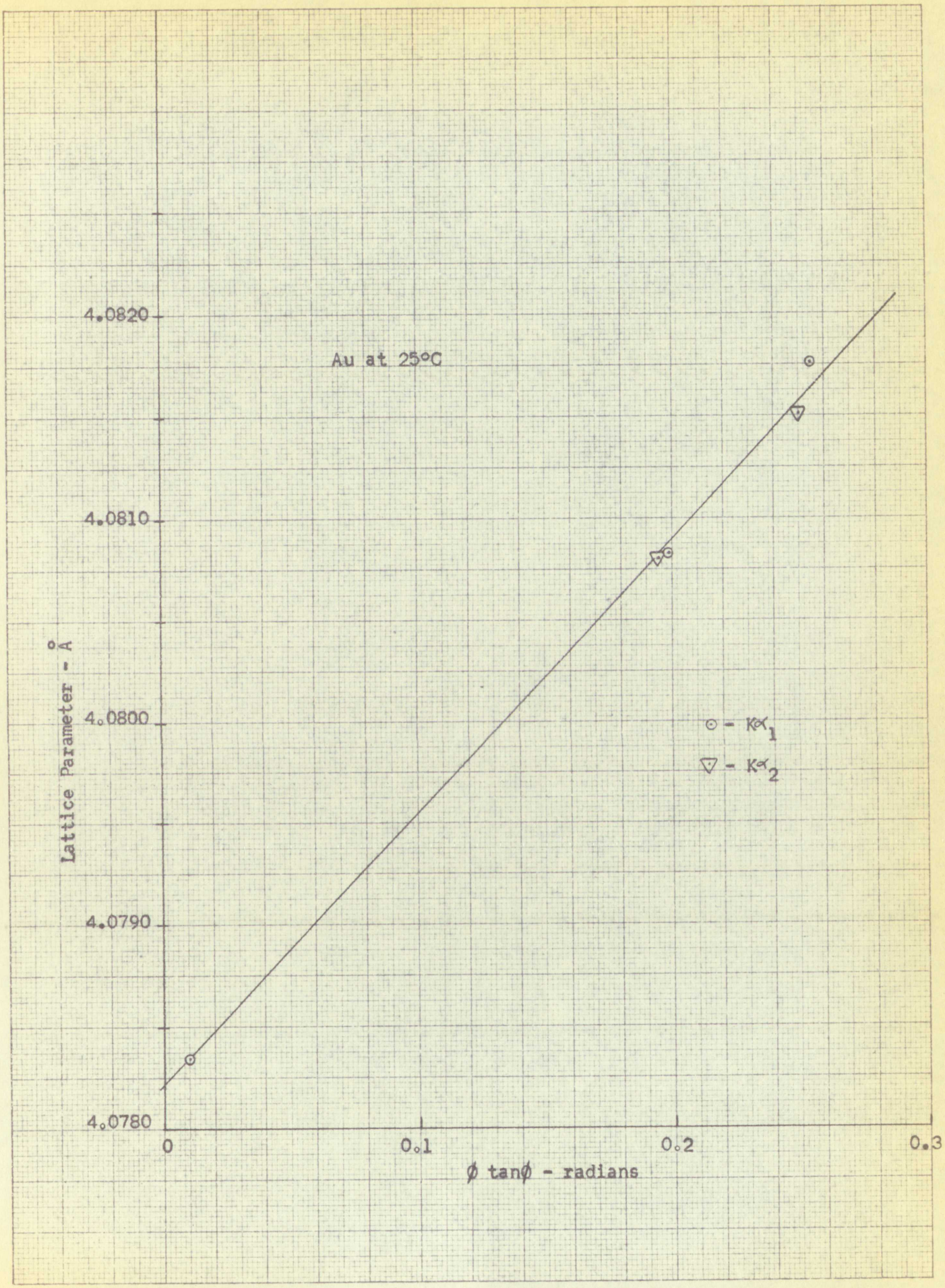

Figure 17. Plot of ø tanø for Au at 25°C from sample calculations to obtain the true lattice parameter.

3.

Lattice Parameter versus Temperature from the Au Internal Standard

The determination of the lattice parameters of MgO versus temperature using the internal standard method is illustrated in the following example.

The raw data obtained from measuring the diffraction lines of MgO and Au produced on the film, shown in Figure 18, are tabulated as follows:

MgO					Au				
h	k	l	K α	S, cm.	h	k	l	K α	S, cm.
4	2	0	1	19.335	3	3	1	1	18.955
4	2	0	2	19.165	3	3	1	2	18.785
4	2	2	1	11.110	4	2	0	1	17.025
4	2	2	2	10.825	4	2	0	2	16.850
4	2	0	1	19.330	4	2	2	1	5.870
4	2	0	2	19.165	4	2	2	2	5.265
4	2	2	1	11.110	3	3	1	1	18.950
4	2	2	2	10.820	3	3	1	2	18.780
4	2	0	1	19.330	4	2	0	1	17.025
4	2	0	2	19.160	4	2	0	2	16.825
4	2	2	1	11.120	4	2	2	1	5.875
4	2	2	2	10.810	4	2	2	2	5.270
					3	3	1	1	18.955
					3	3	1	2	18.775
					4	2	0	1	17.025
					4	2	0	2	16.835
					4	2	2	1	5.870
					4	2	2	2	5.265

Note: Three sets of measurements are presented for better statistics.

λ_1 (Ni $K\alpha_1$) = 1.65784

λ_2 (Ni $K\alpha_2$) = 1.66169

Camera diameter = 19.00 cm.

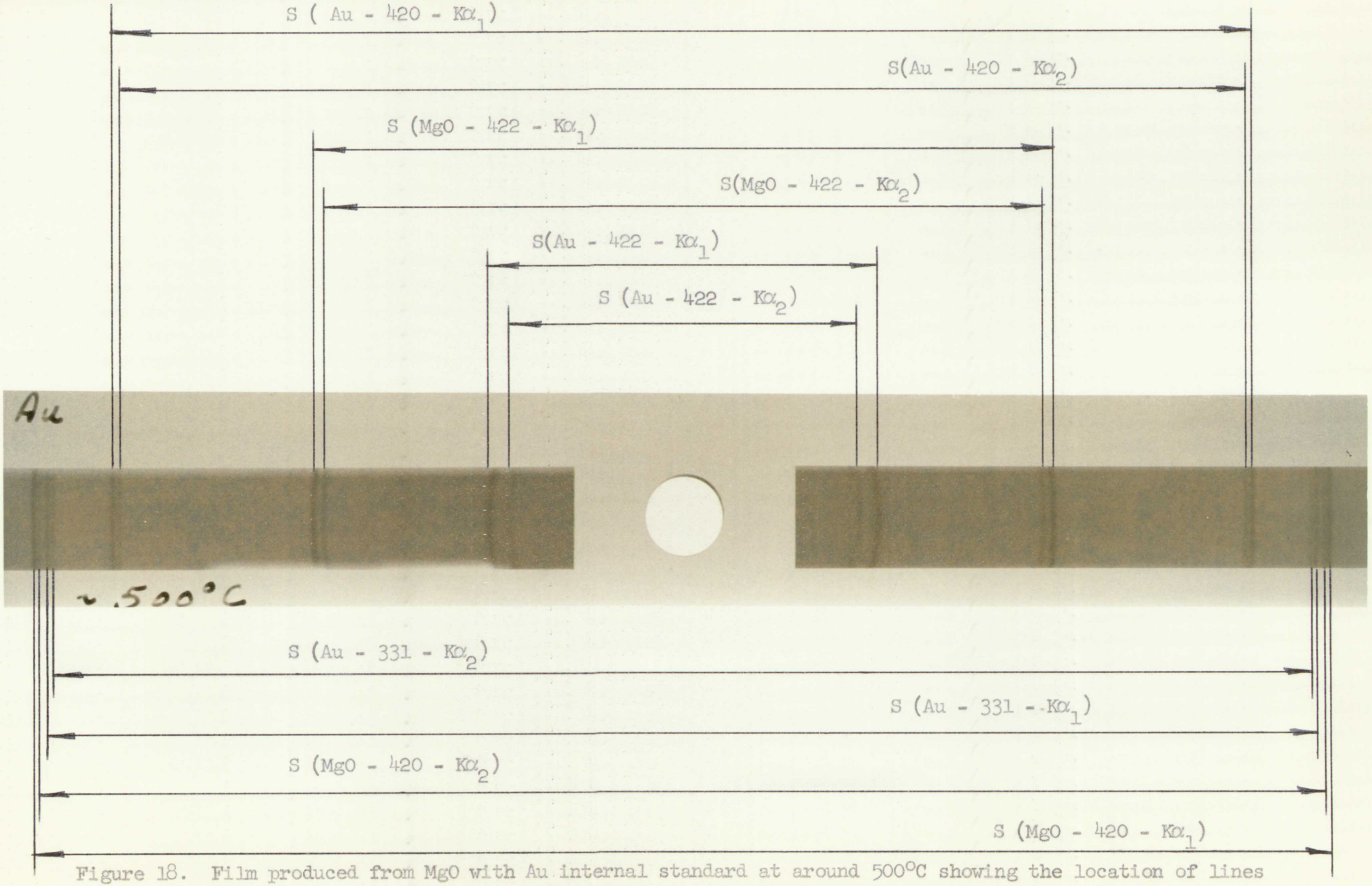

Figure 18. Film produced from MgO with Au internal standard at around 500°C showing the location of lines in the diffraction pattern from which the measurements were taken.

This data is coded for the IBM 704 computer using the Vogel and Kempter method as described in Part 2 above, and the following values for the lattice parameters were obtained:

Lattice parameter, a, for MgO = 4.23953 ± 0.00013 Å

Lattice parameter, a, for Au = 4.10939 ± 0.0005 Å

Using the lattice parameter for Au and referring to the table of lattice parameter versus temperature for Au in the Appendix, we find this lattice parameter for Au corresponds to a temperature of 514°C.

Therefore, the lattice parameter of MgO at 514°C is equal to 4.23953 ± 0.00013 Å.

4.

Percent Linear Thermal Expansion

$$\% = \frac{a_t - a_o}{a_o} \times 100$$

where

% = percent expansion from reference temperature, t_o, to temperature, t, °C

a_t = lattice parameter at temperature, t, °C

a_o = lattice parameter at reference temperature, t_o, °C

Calculating the expansion of MgO from 25-100°C, using the curve of Figure 22 for values of a,

$a_o = 4.2128$ Å at 25°C

$a_t = 4.2163$ Å at 100°C

$$\% = \frac{4.2163 - 4.2128}{4.2128} \times 100 = \underline{0.083}$$

5.

Coefficients of Linear Thermal Expansion

The coefficients of linear thermal expansion were calculated from the lattice parameters corrected for refraction and using quadratic equations derived from least squares analysis of the data.

The mean linear coefficient, $\bar{\alpha}$, which is generally used in thermal stress work, was calculated from the relation,

$$\bar{\alpha} = \frac{1}{a_o} \frac{a - a_o}{t - t_o}$$

where

t_o = reference to temperature

a_o = lattice parameter at the reference temperature

t = temperature

a = lattice parameter at temperature, t

The instantaneous linear coefficient, α_i, and the true linear coefficient, α_t, are of theoretical interest only and were calculated from the following relations,

$$\alpha_i = \frac{1}{a_o} \frac{da}{dt}$$

$$\alpha_t = \frac{1}{a} \frac{da}{dt}$$

The coefficients for Au at 112.8°C were calculated in the following manner:

From the equation for a (corrected for refraction),

$$a = 4.07741 + 5.46458 \times 10^{-5} t + 1.55048 \times 10^{-8} t^2$$

and

$$\frac{da}{dt} = 5.46458 \times 10^{-5} + 3.10097 \times 10^{-8}\ t$$

$$\bar{\alpha} = \frac{1}{a_o}\left[5.46458 \times 10^{-5} + 1.55048 \times 10^{-8}\ (t + t_o)\right] = \frac{1}{4.07855}$$

$$\left[5.46458 \times 10^{-5} + 1.55048 \times 10^{-8}\ (112.8 + 25)\right] = 13.92 \times 10^{-6}/^{o}C$$

$$\alpha_i = \frac{1}{a_o}\ (5.46458 \times 10^{-5} + 3.10097 \times 10^{-8}\ t) = \frac{1}{4.07855}$$

$$(5.46458 \times 10^{-5} + 3.10097 \times 10^{-8} \times 112.8) = 14.26 \times 10^{-6}/^{o}C$$

$$\alpha_t = \frac{1}{a}\,(5.46458 \times 10^{-5} + 3.10097 \times 10^{-8}\ t) = \frac{1}{4.08377}$$

$$(5.46458 \times 10^{-5} + 3.10097 \times 10^{-8} \times 112.8) = 14.24 \times 10^{-6}/^{o}C$$

Values for MgO were calculated in the same manner from the equation,

$$a = 4.21287 + 4.66676 \times 10^{-5}\ (t - 25) + 1.24358 \times 10^{-8}\ (t^2 - 625)$$

(corrected for refraction).

6.

Estimation of Error

In the following calculations, accumulative values are found from the square root of the sum of the squares of independent errors, and the standard deviation, σ, is taken to be equal to one-third of the maximum error, E, unless otherwise stated.

The standard deviations of the lattice parameters due to systematic errors are routinely calculated in the method of Vogel and Kempter[76] and average values for gold and magnesium oxide were as follows:

$$\sigma\,(Au) = 11.5 \times 10^{-5}\ \text{Å}$$

$$\sigma\,(MgO) = 12. \times 10^{-5}\ \text{Å}$$

The standard deviation of temperature for the tables of lattice parameter versus temperature in Appendix I was found as follows:

Standard deviation in temperature measurement for the Pt/Au thermocouple shown below - - - - - - - - - 1.°C

Standard deviation from the least squares analysis of 11 data points- - - - - - - - - - - - - - - - - 1.°C

Accumulative standard deviation, σ - - - - - - - - - 1.4°C

The standard deviation of temperature for the tables of emf versus temperature in Appendix II was found as follows:

Standard deviation of Pt/Au thermocouple (from NBS calibration, E = 1.°C)- - - - - - - - - - - - - - - - 0.3°C

Standard deviation from the least squares analysis of 14 data points - 0.1°C

Accumulative standard deviation, σ - - - - - - - - - 0.4°C

The standard deviation in the temperature measurement for the various phases of the program were estimated as follows:

a. For the thermocouple (Pt/Pt - 10% Rh) method of measuring the thermal expansion of MgO, excluding effects of radiation and conduction which has been treated separately above:

Estimated maximum error of thermocouple - - - - - 3.°C

Maximum error of potentiometer (from specifications)- 0.3°C

Recorded maximum variation of temperature during runs - 5.°C

Accumulative maximum error, E - - - - - - - - - 6.°C

Accumulative standard deviation, σ - - - - - 2.°C

b. For the Pt/Au thermocouple method of measuring the lattice paremeters of Au for the internal standard:

Standard deviation of tables in Appendix II - - - - - - $0.4^{\circ}C$

Estimated maximum temperature error due to the sensitivity of the Au lattice parameter - - - - - - $2.^{\circ}C$

Maximum error of potentiometer (from specifications) - $0.3^{\circ}C$

Recorded maximum variation of temperature during runs - $2.^{\circ}C$

Accumulative maximum error, E - - - - - - - - - - $3.^{\circ}C$

Accumulative standard deviation, σ - - - - - - - - $1.^{\circ}C$

c. For the internal standard method of measuring temperature:

Standard deviation of tables in Appendix I - - - - - - - $1.4^{\circ}C$

Standard deviation of sample temperature during run is estimated from the furnace temperature since there was no thermocouple in the sample during the runs, with E = $2^{\circ}C$ - - - - - - - - - - - - - - - $0.7^{\circ}C$

Accumulative standard deviation, σ - - - - - - - - $1.5^{\circ}C$

The following quadratic equations for the lattice parameters of Au and MgO were derived from a least squares analysis of the data:

$$a\,(Au) = 4.07741 + 5.46458 \times 10^{-5}\, t + 1.55048 \times 10^{-8}\, t^2$$

$$a\,(MgO) = 4.21287 + 4.66676 \times 10^{-5}\,(t - 25) + 1.24358 \times 10^{-8}\,(t^2 - 625)$$

The estimated standard deviation in $\underline{a}$ due to deviations in temperature measurement is found by differentiating $\underline{a}$ with respect to $\underline{t}$, and calculating at the mean of the temperature range or about $500^{\circ}C$:

$$\Delta a\,(Au) = (5.46458 \times 10^{-5} + 3.10097 \times 10^{-8}\, T)\,\Delta T = (5.46458 \times 10^{-5} + 3.10097 \times 10^{-8} \times 500)(1.^{\circ}C) = 7. \times 10^{-5}\ \text{Å}$$

$$\Delta a\,(MgO) = (4.66676 \times 10^{-5} + 2.48716 \times 10^{-8}\, T)\,\Delta t = (4.66676 \times 10^{-5} + 2.48716 \times 10^{-8} \times 500)(1.5^{\circ}C) = 10. \times 10^{-5}\ \text{Å}$$

Accumulative standard deviation in lattice parameters due to systematic and temperature deviations,

$$\sigma(\mathrm{Au}) = 13.5 \times 10^{-5}\ \text{Å}$$

$$\sigma(\mathrm{MgO}) = 15.5 \times 10^{-5}\ \text{Å}$$

The error in the linear expansion coefficient, $\bar{\alpha}$, may be estimated from the following relation at the mean of the temperature range of about 525°C:

$$\bar{\alpha} = \frac{1}{a_o} \frac{a - a_o}{t - t_o}$$

$$(\Delta\bar{\alpha})^2 = \left(\frac{\partial \alpha}{\partial a}\right)^2 (\Delta a)^2 + \left(\frac{\partial \alpha}{\partial t}\right)^2 (\Delta t)^2$$

$$\Delta\bar{\alpha} = \sqrt{\left(\frac{1}{a_o (t - t_o)}\right)^2 (\Delta a)^2 + \left(\frac{a - a_o}{a_o (t - t_o)^2}\right)^2 (\Delta t)^2}$$

$$\Delta\bar{\alpha}(\mathrm{Au}) = \sqrt{\left(\frac{13.5 \times 10^{-5}}{4.0786\ (500)}\right)^2 + \left(\frac{4.1085 - 4.0786}{4.0786\ (500)^2}\right)^2 (1.)^2} = 0.08 \times 10^{-6}/^{\circ}\mathrm{C}$$

$$\Delta\bar{\alpha}(\mathrm{MgO}) = \sqrt{\left(\frac{15.5 \times 10^{-5}}{4.2128\ (500)}\right)^2 + \left(\frac{4.2395 - 4.2128}{4.2128\ (500)^2}\right)^2 (1.5)^2} = 0.07 \times 10^{-6}/^{\circ}\mathrm{C}$$

RESULTS AND DISCUSSION

In the first phase of the study on specimen temperature, it appeared that a thermocouple in contact with the sample should have given greatly improved temperature indication over previous work where the thermocouple was usually located either in the furnace body or "near" the sample. It was surprising to find that the curve obtained in Figure 19 from the data of Table I did not resemble the characteristic concave upward curve of a versus t which one sees in the literature (similar to the dashed curve of Figure 19). Instead, the curve was convex from 25 to 700°C, then it appeared to assume the characteristic shape at the higher temperatures. It was suspected that this resulted from variations in heat transmission since similar effects had been observed by previous authors using thermocouples. Heat transfer calculations showed this to be a reasonable diagnosis when compared with later work as shown in Figure 14. If more complete data on the variation of thermal properties with temperature were available, it is possible that better quantitative agreement could have been obtained. The conduction of the thermocouple and the radiation from the sample appear to equalize the temperatures of thermocouple and sample at about 725°C in Figure 19, while below this value conduction cools the thermocouple below the sample temperature, and above 725°C radiation cools the sample below the thermocouple temperature. The maximum temperature difference shown in Figure 19 was about 85°C at a sample temperature of 400°C.

TABLE I

LATTICE PARAMETER MEASUREMENTS OF MgO

(with Pt/Pt-10% Rh thermocouple in contact with sample)

Temperature, °C	Lattice Parameter,* Å
25.0	4.21283
92.	4.21689
99.5	4.21869
203.	4.22433
312.	4.23149
380.5	4.23644
393.	4.23612
502.5	4.23973
588.	4.24564
588.	4.24579
658.	4.24892
699.5	4.24965
704.	4.25064
716.	4.25116
745.	4.25347
804.	4.25692
815.	4.25685
852.	4.25887
875.	4.25972
888.	4.26033
1002.	4.26735

*Calculated from λ_1 (Ni Kα_1) = 1.65784 Å

λ_2 (Ni Kα_2) = 1.66169 Å

Uncorrected for refraction.

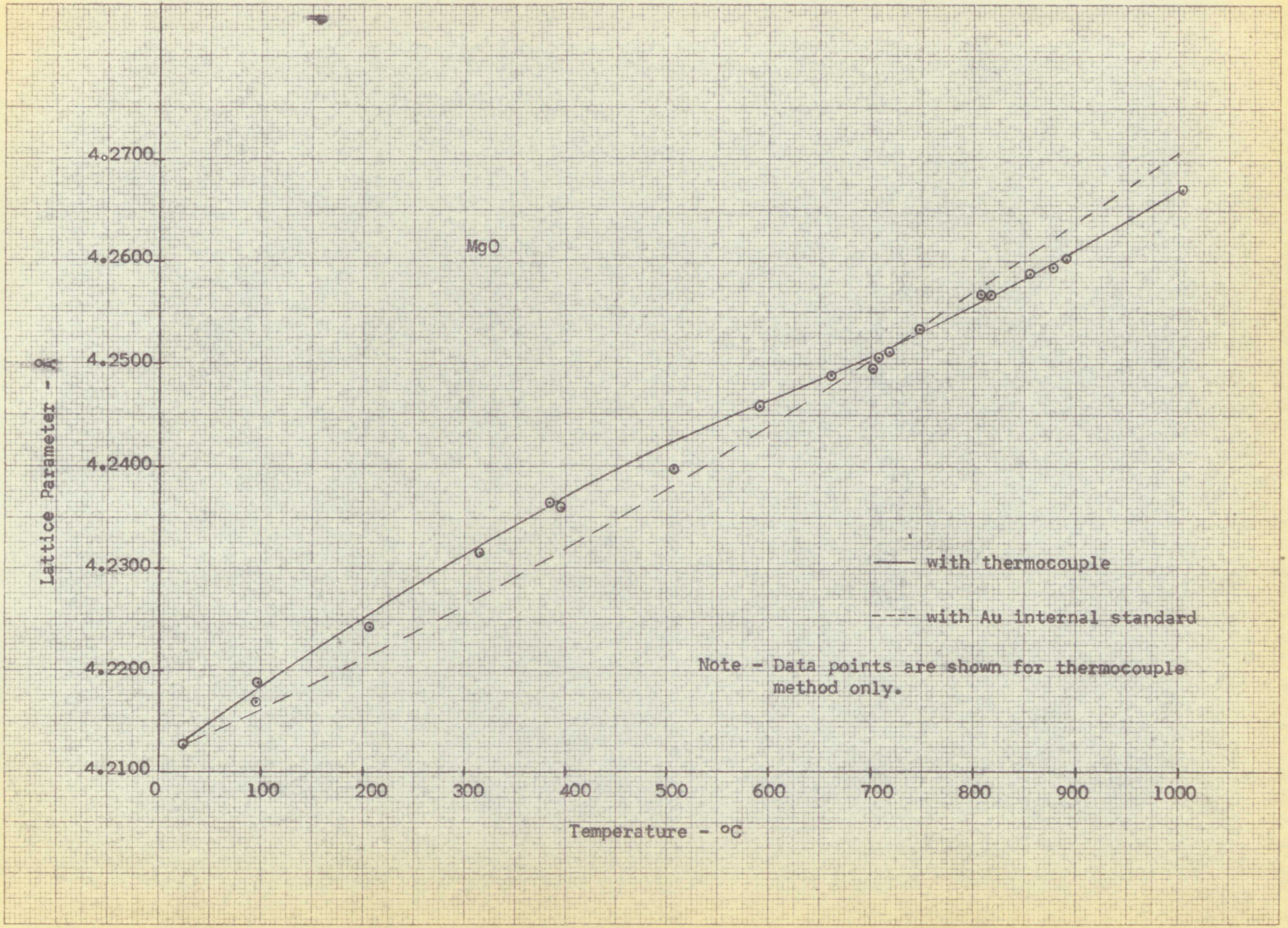

Figure 19. Lattice Parameter vs. Temperature for MgO using thermocouple compared with curve obtained using the Au internal standard.

Looking for another approach, it was decided to adopt the technique of mixing a material of known lattice-temperature relations with the sample with one important refinement. Instead of referring to published lattice-temperature data in which one could not be sure of the lattice parameter precision and (especially) the temperature precision, obtain this data experimentally for a standard material which could serve as both specimen and thermocouple with both being in the irradiating beam. Au was chosen for its inertness, relatively high thermal expansion, and melting point of over 1000°C.

Specially selected Pt/Au thermocouple specimens were calibrated with an accuracy of 1°C by the National Bureau of Standards, and the emf versus temperature tables in Appendix II were compiled from a least squares analysis of their data with an estimated error of about 1°C. The lattice parameters obtained for the Au standard are shown in Figure 20 and Table II with an estimated precision of $\pm$ 13.5 x 10^{-5} Å.

The results obtained by various authors in the literature are shown in Table III and plotted in Figure 21 for comparison. All data was normalized to percent expansion above 25°C unless otherwise noted in the Literature section. It is interesting to note how the points of Esser, Eilender, and Bungardt, who used a thermocouple with X-ray diffraction, closely resemble the deviation obtained here in the initial runs with MgO shown in Figure 19, even to crossing over in the same range of 700-800°C.

Wire specimens suffer grain growth at elevated temperatures which reduces the quality of the film so every effort was made to keep the exposure time to a minimum at the higher temperatures, e.g. above 700°C.

TABLE II

LATTICE PARAMETER MEASUREMENTS OF Au

(with Pt/Au thermocouple specimen in X-ray beam)

Temperature, ^{o}C	Lattice Parameter,* $\overset{o}{A}$
25.0	4.07852
112.5	4.08356
196.	4.08846
312.5	4.09589
502.	4.10856
610.	4.11619
645.	4.11878
700.	4.12301
808.	4.13122
910.	4.13980
1002.	4.14795

*Calculated from λ_1 (Ni $K\alpha_1$) = 1.65784 $\overset{o}{A}$

λ_2 (Ni $K\alpha_2$) = 1.66169 $\overset{o}{A}$

Uncorrected for refraction.

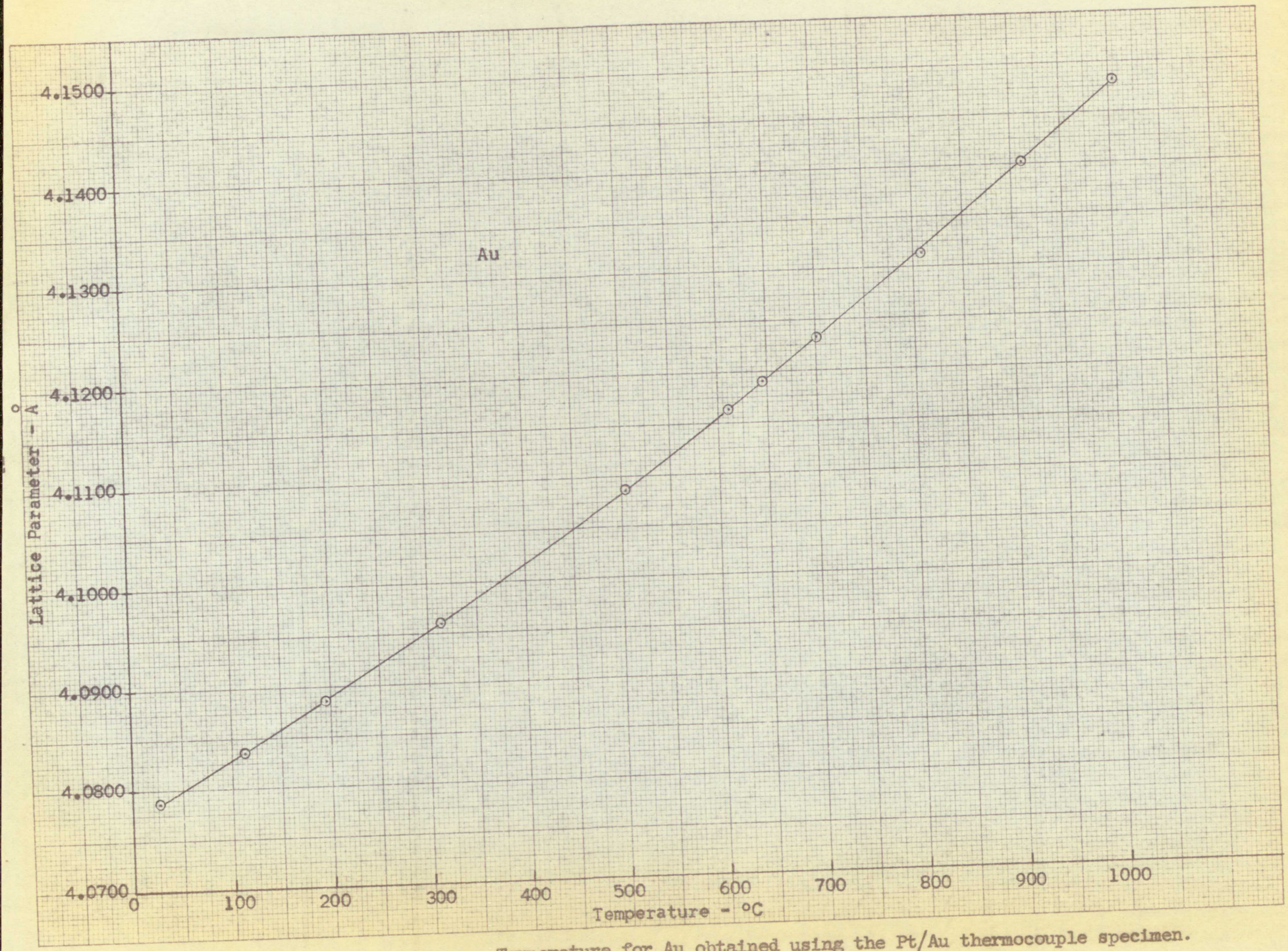

Figure 20. Lattice Parameter vs. Temperature for Au obtained using the Pt/Au thermocouple specimen.

TABLE III

COMPARISON OF THE LINEAR THERMAL EXPANSION OF Au
OBTAINED BY VARIOUS AUTHORS

Author and Reference	Percent Expansion Above Room Temperature									
TEMP.	100	200	300	400	500	600	700	800	900	1000
Müller (43)	0.1078	0.2567	0.4085	0.5646	0.7273	0.8925	1.062	1.236	1.415	1.598
Austin (44)	.1068	.2541	.4049	.5610	.7256	.8952	1.073	1.258	1.454	
Bungardt (47)	.1226	.2820	.4316	.5909	.7503	.9220	1.106	1.277	1.461	1.672
Nix (48)	.106	.251	.405	.562	.724	.897	1.067			
Esser (49)	.1158	.2574	.4033	.5541	.7110	.8742	1.0444	1.2222	1.4091	
Gott (50)	.095	.248	.397	.538						
Merryman	.103	.248	.402	.562	.731	.907	1.09	1.28	1.48	1.69

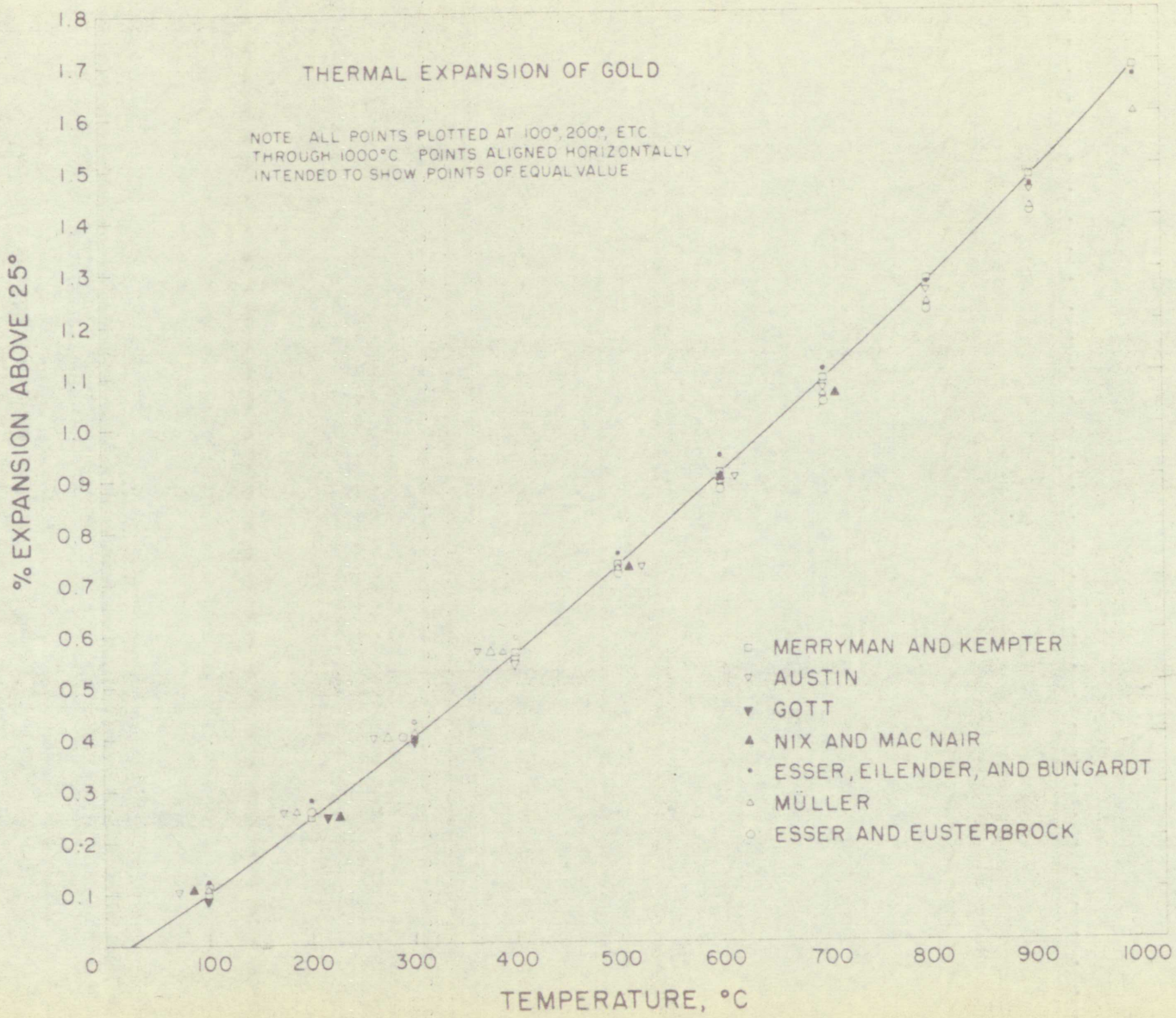

Figure 21. Comparison of the linear thermal expansion of Au obtained by various authors.

A fine grain Au plate would eliminate this problem and was tried in the course of this work. Although the pattern on the film improved, a relatively high impurity of copper in the Au plate decreased the lattice parameter of the Au being measured so that the results could not be used. The analyses of the Au and Pt wire used, and the Au plating are shown in Table VI. Although the amount of copper impurity shown appears to be small, this value when used in the equation of Zen[81] gives the same decreased lattice parameter for Au as was measured by X-ray diffraction. The thermocouple formed by the 3 mil Pt wire brazed to the surface of the 10 mil Au specimen is measuring the surface temperature of the specimen. Considering the attenuation of Au in Appendix IV where the half-thickness is about 0.06 mils, the temperature indicated is also the temperature of that portion of the specimen (e.g. the surface) from which the lattice parameters are derived.

When the lattice parameters of MgO were subsequently measured with temperature indication from the Au standard developed above, values were obtained with an estimated precision of $\pm$ 15.5 x 10^{-5} ^{o}A. Analyses of the powdered MgO and Au used are shown in Table VI. The expected concave upward curve was obtained in Figure 22 plotted from the data in Table IV. Again the results are compared with those of other authors in Table V and Figure 23. While not a proof of accuracy, the fact that the curve from this work passes through the approximate statistical average of all other points is an indication of the improved quality of the data.

From the Interlaboratory Study on Thermal Expansion of MgO conducted by the Bureau of Mines, the results submitted from this work were in good agreement with those of others who used internal standards. Best agreement

TABLE IV

LATTICE PARAMETER MEASUREMENTS OF MgO

(with internal Au standard calibrated with Pt/Au thermocouple specimen in X-ray beam)

Temperature, °C	Lattice Parameter,* Å
25.0	4.21282
116.	4.21703
241.	4.22323
303.	4.22644
367.	4.23020
444.	4.23479
514.	4.23953
570.	4.24234
627.	4.24623
637.	4.24647
696.	4.25052
774.	4.25517
865.	4.26136
932.	4.26553

*Calculated from λ_1 (Ni Kα_1) = 1.65784 Å

λ_2 (Ni Kα_2) = 1.66169 Å

Uncorrected for refraction.

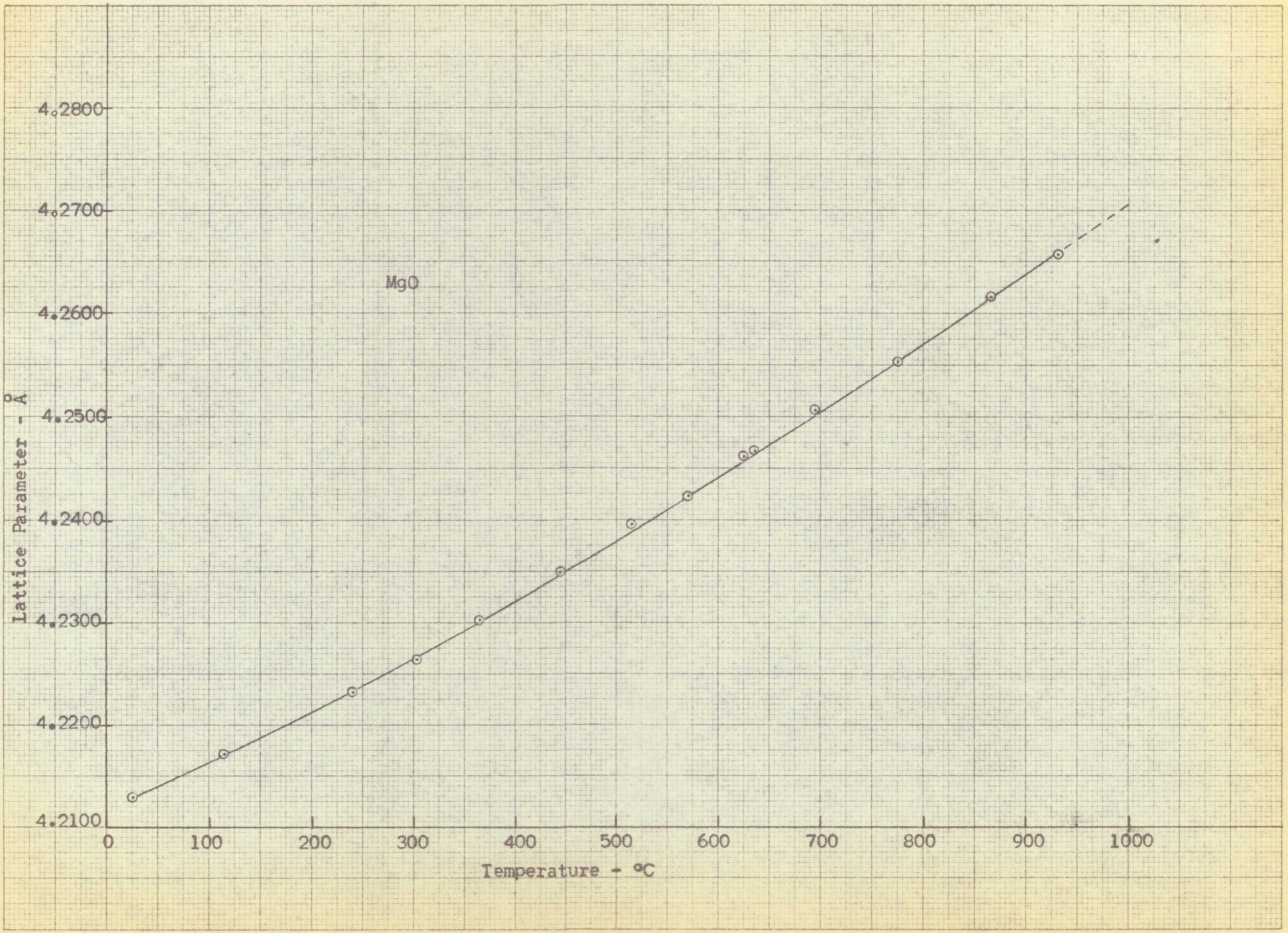

Figure 22. Lattice Parameter vs. Temperature for MgO using the Au internal standard.

TABLE V

COMPARISON OF THE LINEAR THERMAL EXPANSION OF MgO

OBTAINED BY VARIOUS AUTHORS

Author and Reference	Expansion Above Room Temperature									
TEMP	100	200	300	400	500	600	700	800	900	1000
Rieke (54)		0.200		0.462	0.599	0.741	0.883			
Bogitch (55)		.20		.53		.81		1.19		1.57
Thilenius (56)		.207		.350		.755		1.07		1.39
Austin (58)	0.073	.196	0.325	.462	.607	.752	.900	1.05	1.20	1.35
Kanz (57)	.093	.213	.337	.479	.616	.751	.909	1.064	1.230	1.388
Meindl (59)		.2		.4		.65		1.0		1.2
Büssem (60)			.370		.607		.890			1.40
Ebert (61)			.324		.592		.893		1.20	1.36
Durand (62)	.070	.183								
White (63)	.1270	.2430	.3808	.5089	.5865	.7355	.8801	1.0249	1.1680	1.3334
Pole (64)		.15		.40		.60		.90		1.1
Sharma (66)	.091	.210	.335	.467		.753		1.10		
Schwartz (67)		.18		.45		.75		1.05		1.35
Mauer (25)		.200		.472		.744		1.04		1.36
Beals (69)		.255		.490		.765		1.032		1.33
Zimmerman (29)		.213		.405		.750		1.04		1.30
Whittemore (70)			.366			.776			1.22	
Skinner (32)	.065	.185	.305	.440	.580	.717	.860			
Klein (72)		.180		.410		.830		1.25		1.59
Campbell (42)		.25		.50		.80		1.10		1.45
Fieldhouse (74)	.09	.21	.30	.48	.60	.75	.88	1.03	1.16	1.34
Merryman	.083	.195	.325	.456	.598	.752	.895	1.049	1.208	1.370

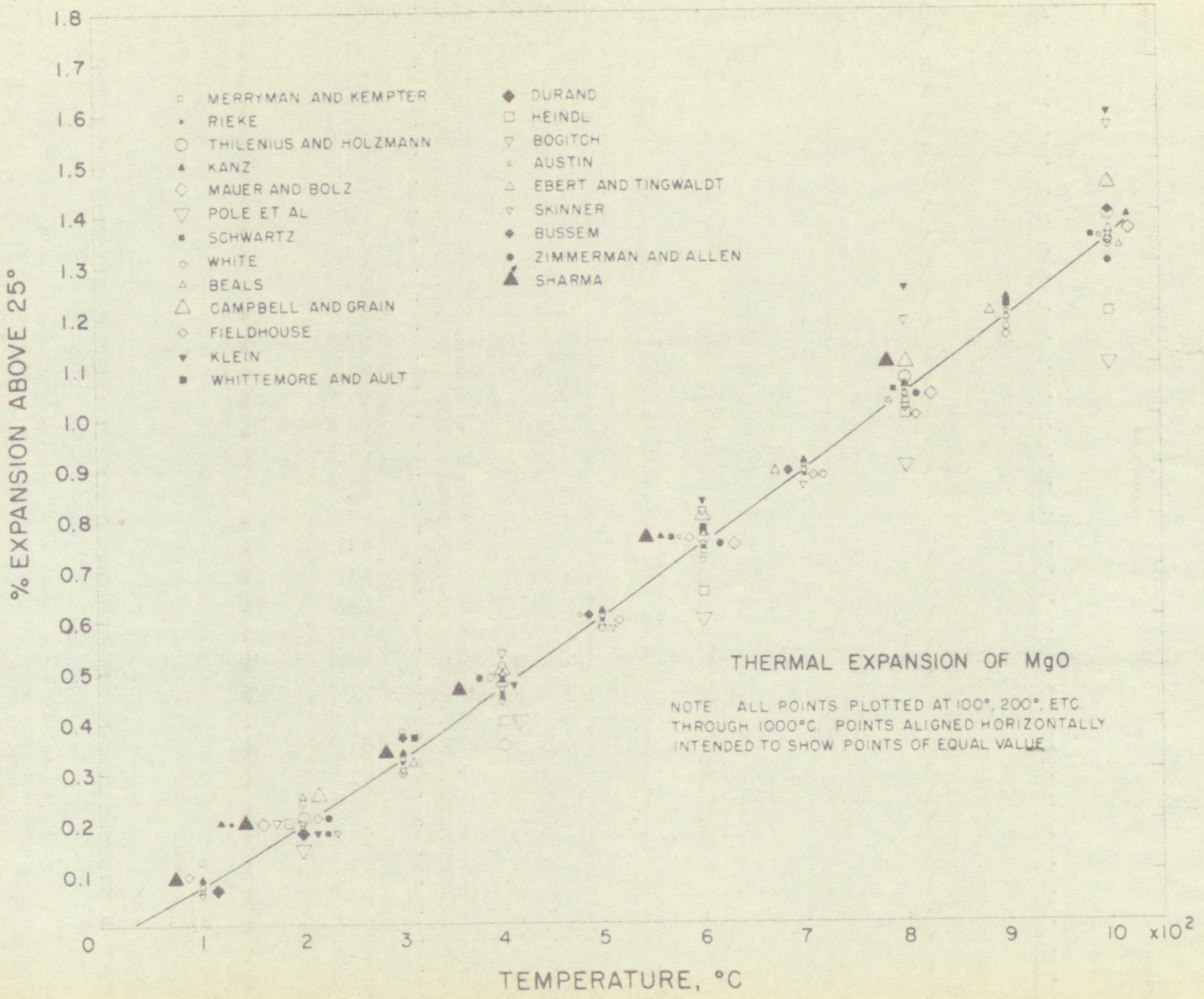

Figure 23. Comparison of the linear thermal expansion of MgO obtained by various authors.

TABLE VI

SPECTROCHEMICAL ANALYSIS RESULTS

(ppm unless otherwise stated)

Impurity	MgO (B. of M.)	Au (Powder)	Au (.010" Wire)	Pt (.003" Wire)	Au Plate* (on Pt/Au t'ople)
Li	1	20	20	40	ND
Be	1	10	10	10	ND
B	100	40	40	100	ND
Na	3	100	100	40	0.01 - 0.1
Mg		10	10	100	0.01 - 0.1
Bi	3				ND
Al	20	100	100	200	ND
Si	300	10-100			.001 - .01 o/o
K	10	400	200		.001 - .01 o/o
Ca	0.3 o/o	100	100	100	.01 - .1 o/o
Ti	200	ND			ND
V	10	400	400	400	ND
Cr	50	100	100	100	ND
Mn	200	40	40	100	ND
Fe	200	100	100	200	.001 - .01 o/o
Co	3	400	400	100	ND
Ni	10	100	100	100	ND
Cu	10	10	40	40	.1 - 1 o/o
Zn	30	ND	0.1 o/o		ND
Sr	10	200	200	100	ND
Mo	3	ND		ND	ND
Ru		0.1 o/o	100	0.4 o/o	ND
Rh		0.1 o/o	0.1 o/o	400	ND
Pd		100	100	100	ND
Ag	1	10	10-100 (est.)		.001 - .01 o/o
Cd	10	400	400		ND
Sn	10	ND		ND	ND
Ba	10	100	100	100	ND
Ir		0.1 o/o	0.1 o/o	400	ND
Pt		100	100	Major	1 - 10 o/o
Au		Major	Major	100	10 o/o
Pb	10	400	40		ND

*estimated amounts
ND = Not Detected

was with Brand and Goldschmidt at the lower temperatures, while at higher temperatures their values tend to lower values of percent expansion than the curve, being about 0.1% lower at 1200°C. Since the "last lines" method used by Brand and Goldschmidt is not a precision method of calculating lattice parameters, it is impossible to speculate on this deviation. The report[32] concludes, "The average difference between observed and tabulated values over the temperature range 500°C to 1200°C is approximately 1, 2, and 2 percent for X-ray cameras, X-ray diffractometers, and dilatometers, respectively. Below 500°C X-ray camera values show a significantly lower dispersion than the other methods. Five laboratories (D, E, F, M*, and P), using either X-ray camera or X-ray diffractometer methods, employed internal standards as a means of thermal calibration; gold, silver, iron, or platinum being used. Their values for magnesium oxide are in close agreement to those tabulated from constants derived from X-ray camera data only." (See curve in Appendix III.)

The coefficient of linear thermal expansion for MgO and Au were calculated from the data obtained in the course of the thesis and are shown in the curves of Figures 24 and 25. The standard deviation of the average coefficient is estimated to be $\pm$ 0.07 x 10^{-6}/°C for MgO, and $\pm$ 0.08 x 10^{-6}/°C for Au. Although the instantaneous and true coefficients are not of importance to the objective of this thesis, they have been included for their theoretical interest.

At the start of this work, the goal was to obtain temperature measurements to a precision of $\pm$ 1°C. This was not attained where the thermocouple

---

*R. G. Merryman and C. P. Kempter, University of California, Los Alamos Scientific Laboratory, Los Alamos, New Mexico (from data of this thesis).

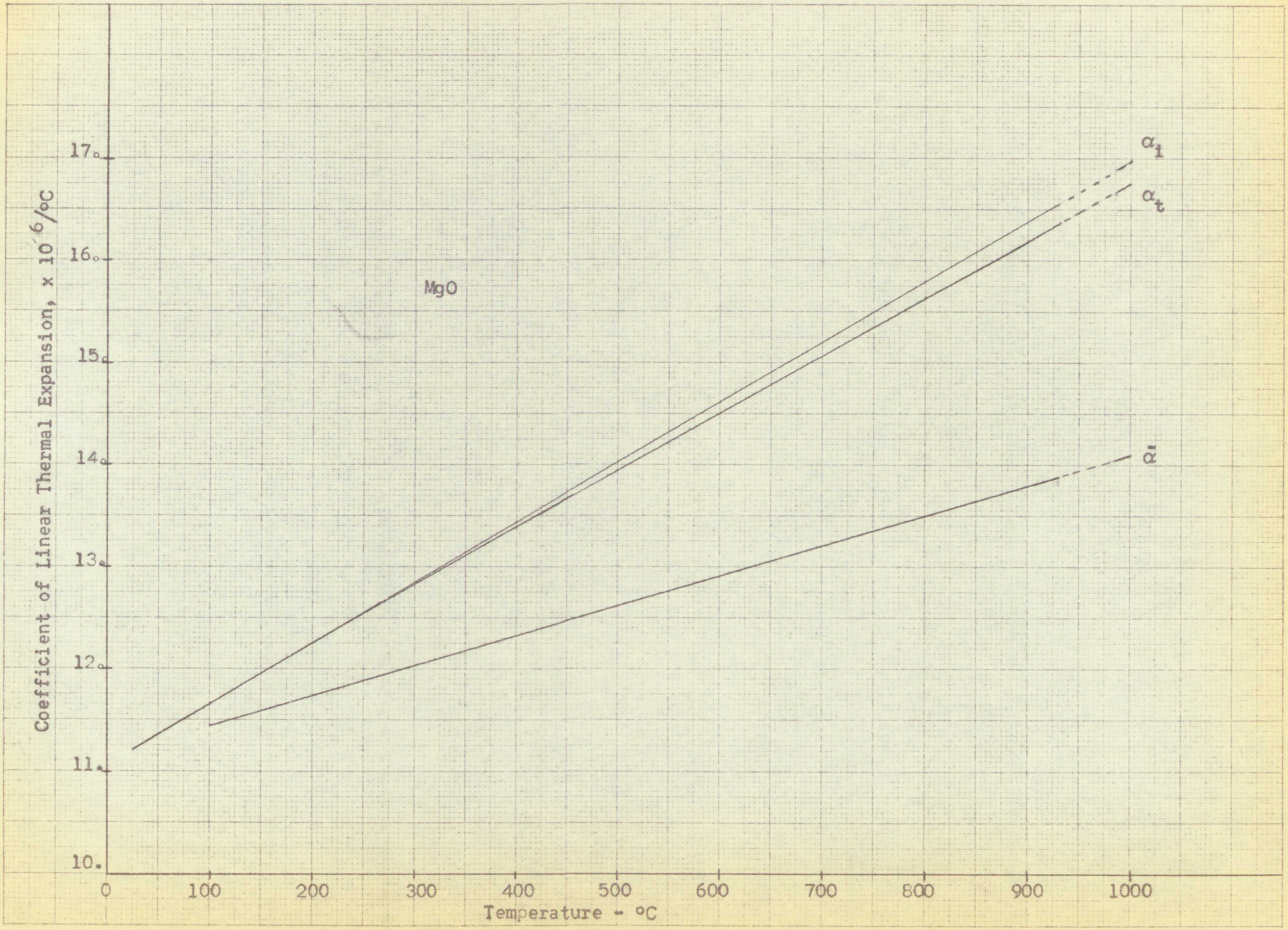

Figure 24. The coefficients of linear thermal expansion for MgO.

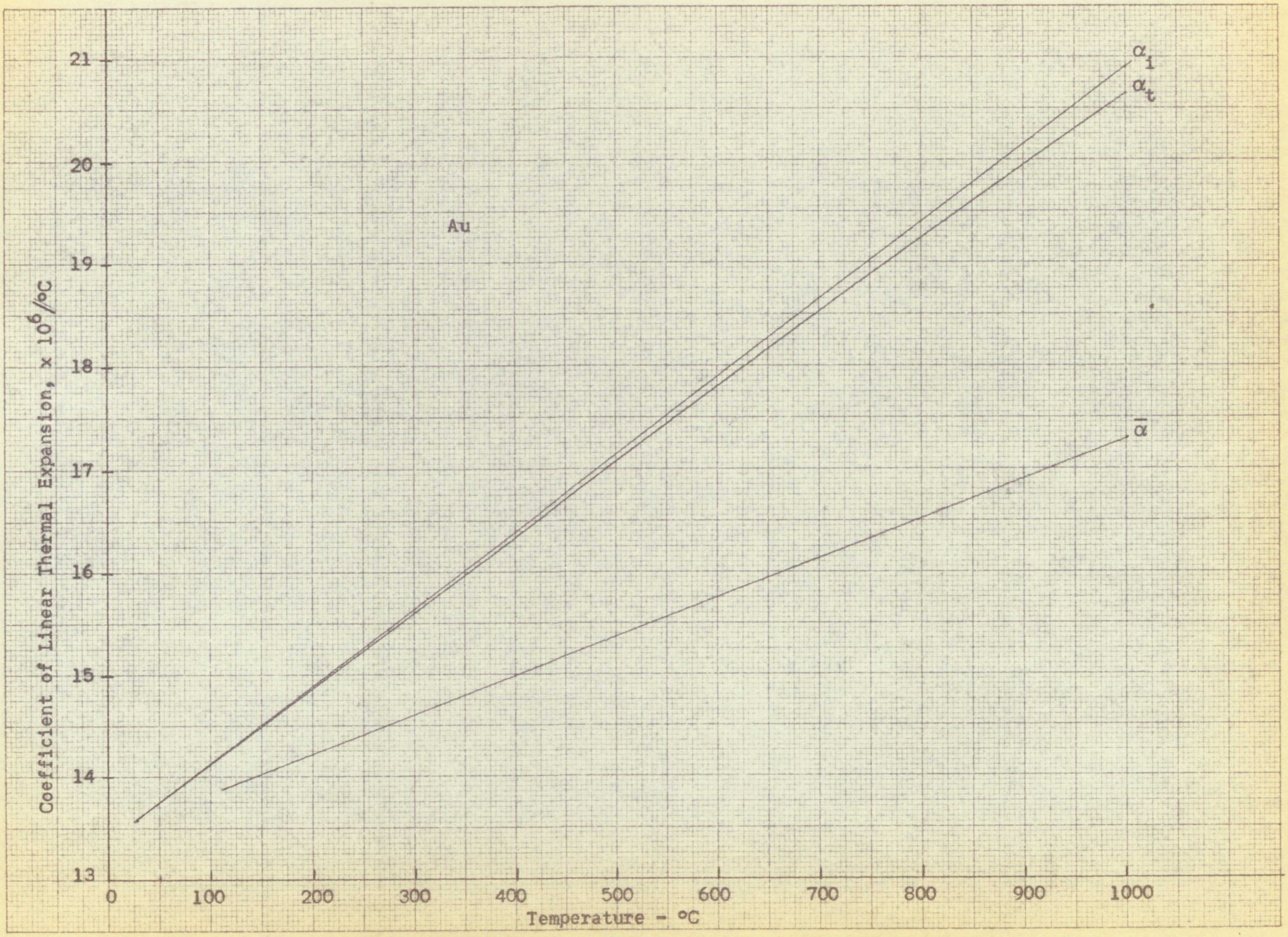

Figure 25. The coefficients of linear thermal expansion for Au.

was used because errors as high as 85°C were experienced due to conduction and radiation effects on the thermocouple and sample as described in detail above. In the case of the Au internal standard, this degree of precision was found impossible because the change in lattice parameter for Au could not be detected with a change in temperature of less than about 2°C. In this connection, in addition to the lack of thermal properties for powders previously mentioned in the calculations, it should be pointed out that the temperature effects in the mixture of MgO and Au powders are unknown. It is certainly possible that the MgO and Au particles could be at different temperatures due to their difference in thermal conductivity and emissivity, in which case the temperature derived from the Au standard would be in error with reference to the MgO sample.

SUMMARY OF ESTIMATED ERRORS

Temperature by the thermocouple method, maximum	85°C
Temperature by the Au internal standard method, σ	1.5°C
Lattice parameter of Au, σ	13.5×10^{-5} Å
Lattice parameter of MgO, σ	15.5×10^{-5} Å
Average Coefficient of Linear Thermal Expansion of Au, σ	0.08×10^{-6}/°C
Average Coefficient of Linear Thermal Expansion of MgO, σ	0.07×10^{-6}/°C

CONCLUSIONS AND RECOMMENDATIONS

1. Selected materials can be calibrated to give precise temperature measurements in Debye-Scherrer specimens during high temperature X-ray diffraction measurement of thermal expansion. The method of calibration is based on using the specimen as one leg of the thermocouple with both the specimen and the thermocouple junction located in the path of the X-ray beam. The Au standard developed in the thesis will measure temperatures from 25 to 1000°C with a precision of 1.5°C.

2. The lattice parameters of Au and MgO can be precisely measured from room temperature to about 1000°C with an average precision of 13.5 x 10^{-5} Å and 15.5 x 10^{-5} Å, respectively.

3. The coefficients of linear thermal expansion for Au and MgO were determined from the lattice parameters with an average precision of 0.08 x 10^{-6}/°C and 0.07 x 10^{-6}/°C, respectively.

4. The use of a thermocouple to measure the temperature of Debye-Scherrer specimens has been shown to give errors as high as 85°C.

5. The method described using an internal standard of Au (or some other selected material) for temperature measurement is recommended for the measurement of temperature in Debye-Scherrer specimens during high temperature X-ray diffraction.

6. Although the internal standard method appears to be adequate for temperature measurement, the thermal properties of powdered materials and mixtures would be helpful in evaluating the possible uncertainty in the internal standard method mentioned previously.

REFERENCES

1. Westgren, A., J. Iron and Steel Inst. (London) 103, 303 (1921).

2. Becker, K., Z. f. Phys. 40, 37 (1926).

3. Cohn, W. M., Z. f. Phys. 50, 123 (1928).

4. Jay, A. H., Proc. Phys. Soc. London 45, Part 5, No. 250, 635 (1933).

5. Dorn, J. E., and Glocker, G., Rev. Sci. Instr. 17, 389 (1936).

6. Hume-Rothery, W., and Reynolds, P. W., Roy. Soc. London, Proceedings, 167, Seties A, 25 (1938).

7. Ellwood, E. C., J. Inst. Metals, Vol. 66, 87 (1940).

8. Wilson, A. J. C., Proc. Phys. Soc. London 53, 235 (1941).

9. Birks, L. S., and Friedman, H., Nav. Res. Lab. Rep. N-3081 (1947).

10. Van Valeenburg, A., Jr., and McMurdie, H. F., J. Nat'l Bur. Stds., 38, 415 (1947).

11. Alcock, T. C., Peiser, H. S., and Swallow, H. T. S., J. Sci. Instr. 24, 297 (1947).

12. Gordon, P., J. Applied Phys. 20, 908 (1949).

13. Edwards, J., Speiser, R., and Johnston, H., Rev. Sci. Instr. 20, 343 (1949).

14. Goldschmidt, H. J., and Cunningham, J., J. Sci. Instr. 27, 177 (1950).

15. Williams, E. C., J. Sci. Instr. 27, 154 (1950).

16. Mueller, M. H., and Zauberis, D. D., Argonne Nat'l Laboratory Report ANL-FF-306a.

17. Berry, R. L., Henry, W. G., and Raynor, G. V., J. Inst. Metals 78, 643 (1951).

18. Basinski, Z. S., Pearson, W. B., and Christian, J. W., J. Sci. Instr. 29, 154 (1952).

19. Mauer, F. A., and Bolz, L. H., Nat'l Bur. Stds. Report 3148, 39 (1953).

20. Birks, L. S., Rev. Sci. Instr. 25, No. 10, 963 (Oct. 1954).

21. Johnson, J. R., J. Am. Ceram. Soc. 37, 360 (1954).

22. Pease, R. S., J. Sci. Instr. 32, 476 (Dec. 1955).

23. Matuyama, E., J. Sci. Instr. 32, 229 (June 1955).

24. Mauer, F. A., and Bolz, L. H., Nat'l Bur. Stds. Report WADC-TR-55-473, (Dec. 1955).

25. Basinski, Z. S., and Hume-Rothery, W., Proc. Roy. Soc. A229, 459 (1955).

26. Brand, J. A., and Goldschmidt, H. J., J. Sci. Instr. 33, 41 (1956).

27. Kuznetsov, V. G., Zhurnal Neorganicheskoi Khimii 12, 1548 (1956).

28. Zimmerman, W. F., and Allen, A. W., Amer. Cer. Bull. 35, 271 (1956).

29. Fridrichsons, J., Rev. Sci. Instr. 27, No. 12, 1015 (Dec. 1956).

30. Austin, A. E., Richard, H. A., and Schwartz, C. M., Rev. Sci. Instr. 27, 860 (1956).

31. Skinner, B. J., Am. Mineralogist (J. Min. Soc. Am.) 42, 39 (1957).

32. Goon, E. J., Mason, J. T., Gibb, T. R., Jr., Rev. Sci. Instr. 28, 343 (1957).

33. Gindin, Ye. I., and Prokhvatilov, V. G., Zavodskaya Lab. 24, No. 1, 106 (1958).

34. Hanak, S. S., Dissertation for PhD in Physical Chemistry, Iowa State Univ. (546. 9-H233h) (1959).

35. Aruja, E., Welch, J. H., and Gutt, J. Sci. Instr. 36, 1 (1959).

36. Spreadborough, J., and Christian, J. W., J. Sci. Instr. 36, 116 (1959).

37. Van Niekerk, J. N., J. Sci. Instr. 37, 172 (May 1960).

38. Simmons, R. O., and Balluffi, R. W., Phys. Rev. 119, 600 (1960).

39. Simmons, R. O., and Balluffi, R. W., Phys. Rev. 117, 52 (1960).

40. Das, D. K., Instr. Control Systems 33, No. 12, 2085 (Dec. 1960).

41. Intrater, J., and Hurwitt, S., Rev. Sci. Instr. 32, No. 8, 905 (1961).

42. Campbell, W. J., and Grain, C., Report BM-RI-5757 (1960).

43. Müller, von Alex., Physik. Z. 17, 29-30 (1916).

44. Austin, J. B., Physics 3, 240 (1932).

45. Shinoda, G., Proc. Phys-Math. Soc. Japan 16, 436-8 (1934).

46. Rose, T. K., and Newman, W. A. C., "The Metallurgy of Gold," Charles Griffin Company, London (1937), p. 6.

47. Esser, H., Eilender, W., und Bungardt, K., Archiv fur das Eisenhuttenwesen 12, 157-61 (1938).

48. Nix, F. C., and MacNair, D., Phys. Rev. 60, 597-605 (1941).

49. Esser, J., and Eusterbrock, H., Archiv fur das Eisenhuttenwesen 14, 341-55 (1941).

50. Gott, A., Ann. Phys. Lpz. (V) 41, 520 (1942).

51. Swanson, H. E., and Tatge, E., Nat'l Bur. Stds. Circular 539, Vol. I (1953).

52. Krikorian, O. H., Report UCRL-6132 (1960).

53. Goodwin, H. M., and Mailey, R. D., Trans. Am. Electrochem. Soc. 9, 89-98 (1906).

54. Rieke, R., Keram. Rundsh. 12, S. 143 (1914).

55. Bogitch, M. B., Compt. rend. 173, 1358-60 (1921).

56. Thilenius, R., and Holzmann, H., Z. f. Anorg. Allg. Chem. 189, 381 (1930).

57. Kanz, A., Mitt. Forsch. Inst. Ver Stahlwerke AKT ges Dortmund, Vol. 2, No. 5, p. 77-96 (1931).

58. Austin, J. B., J. Am. Chem. Soc. 14, 795 (1931).

59. Heindl, R. A., J. Res. Nat. Bur. Stds. 10, 715 (1933).

60. Bussem, W., Ber. deut. keram. Ges. 16, 381-92 (1935).

61. Ebert, H., and Tingwaldt, C., Physik Z. 37, 471 (1936).

62. Durand, M. A., Physics 7, 297-8 (1936).

63. White, H. E., J. Am. Ceram. Soc. 21, 216-229 (1938).

64. Pole, G. R., Beinlich, A. W., Jr., and Gilbert, Nathan, J. Am. Ceram. Soc. 29, 208-22 (1946).

65. Gangler, J. S., Robards, C. F., and McNutt, J. E., Report NACA-TN-1911 (1949).

66. Sharma, S., Proc. Indian Acad. Sci. 32, 268 (1950).

67. Schwartz, G., J. Am. Ceram. Soc. 35, 325-33 (1952).

68. Crandall, W. B., Report WADC-TR-52-327 (1952).

69. Beals, R. J., Dissertation for PhD in Engineering, Univ. of Illinois (1955).

70. Whittemore, O. J., Jr., and Ault, Neil N., J. Am. Ceram. Soc. 39, 443 (1956).

71. Engberg, C. J., and Zehms, E. H., Report USAEC, NAA-SR-3086 (1958).

72. Klein, D. J., Report NAA-SR-2542 (1958).

73. "Refractory Grain Properties and Applications," Norton Company, Form 1741-6PCMX-7-61-CP.

74. Fieldhouse, I. B., and Lang, J. I., Report WADD-TR-60-904 (1961).

75. Stover, C. M., Report SCTM 170-57-52 (1957).

76. Vogel, R. E., and Kempter, C. P., Los Alamos Scientific Laboratory, Report LA-2317 (1959); Acta Cryst. 14, 1130 (1961).

77. Kingery, W. D., "Property Measurements at High Temperatures," John Wiley and Sons, 1959.

78. McAdams, W. H., "Heat Transmission," McGraw-Hill Company, 1954.

79. Clarke, L., "Manual for Process Engineering Calculations," McGraw-Hill Company, 1947.

80. Kempter, C. P., Los Alamos Scientific Laboratory, Report LA-2308 (1959).

81. Zen, E., Am. Mineralogist 41, 523 (1956).

82. Campbell, W. J., "Results of Interlaboratory Study on Thermal Expansion of Magnesium Oxide," to be published.

APPENDIX I

(Note: Lattice parameters are not corrected for refraction.)

TEMPERATURE VS. LATTICE PARAMETER FOR GOLD

Å	.0000	.0001	.0002	.0003	.0004	.0005	.0006	.0007	.0008	.0009
					DEGREES C					
4.077	-----	-----	0.4	2.3	4.1	5.9	7.7	9.6	11.4	13.2
4.078	15.0	16.8	18.6	20.4	22.2	24.1	25.8	27.7	29.5	31.3
4.079	33.1	34.8	36.6	38.4	40.2	42.0	43.8	45.6	47.4	49.1
4.080	50.9	52.7	54.5	56.2	58.0	59.9	61.6	63.3	65.0	66.8
4.081	68.6	70.4	72.1	73.9	75.6	77.4	79.1	80.9	82.6	84.4
4.082	86.1	87.9	89.6	91.4	93.1	94.8	96.6	98.3	100.0	101.8
4.083	103.5	105.2	106.9	108.7	110.4	112.1	113.8	115.5	117.3	119.0
4.084	120.7	122.4	124.1	125.8	127.5	129.2	130.9	132.6	134.3	136.0
4.085	137.7	139.4	141.1	142.8	144.5	146.2	147.9	149.6	151.2	152.9
4.086	154.6	156.3	158.0	159.6	161.3	163.0	164.7	166.3	168.0	169.7
4.087	171.4	173.0	174.7	176.3	178.0	179.7	181.3	183.0	184.6	186.3
4.088	187.9	189.6	191.3	192.9	194.5	196.2	197.8	199.5	201.1	202.8
4.089	204.4	206.0	207.7	209.3	211.0	212.6	214.2	215.8	217.5	219.1
4.090	220.7	222.4	224.0	225.6	227.2	228.8	230.5	232.0	233.7	235.3
4.091	236.9	238.5	240.1	241.7	243.4	245.0	246.6	248.2	249.8	251.4
4.092	253.0	254.6	256.2	257.8	259.4	261.0	262.5	264.1	265.7	267.3
4.093	268.9	270.5	272.1	273.7	275.2	276.8	278.4	280.0	281.6	283.1
4.094	284.7	286.3	287.9	289.4	291.0	292.6	294.1	295.7	297.3	298.8
4.095	300.4	302.0	303.5	305.1	306.6	308.2	309.8	311.3	312.9	314.4
4.096	316.0	317.5	319.1	320.6	322.2	323.7	325.2	326.8	328.3	329.9
4.097	331.4	333.0	334.5	336.0	337.6	339.1	340.6	342.2	343.7	345.2
4.098	346.8	348.3	349.8	351.3	352.9	354.4	355.9	357.4	358.9	360.5
4.099	362.0	363.5	365.0	366.5	368.0	369.6	371.1	372.6	374.1	375.6
4.100	377.1	378.6	380.1	381.6	383.1	384.6	386.1	387.6	389.1	390.6
4.101	392.1	393.6	395.1	396.6	398.1	399.6	401.1	402.6	404.1	405.5
4.102	407.0	408.5	410.0	411.5	413.0	414.4	415.9	417.4	418.9	420.4
4.103	421.8	423.3	424.8	426.3	427.7	429.2	430.7	432.1	433.6	435.1
4.104	436.5	438.0	439.5	440.9	442.4	443.9	445.3	446.8	448.2	449.7
4.105	451.1	452.6	454.1	455.5	457.0	458.4	459.9	461.3	462.8	464.2
4.106	465.7	467.1	468.6	470.0	471.4	472.9	474.3	475.8	477.2	478.6
4.107	480.1	481.5	483.0	484.4	485.8	487.3	488.7	490.1	491.6	493.0
4.108	494.4	495.8	497.3	498.7	500.1	501.5	503.0	504.4	505.8	507.2
4.109	508.6	510.1	511.5	512.9	514.3	515.7	517.1	518.6	520.0	521.4
4.110	522.8	524.2	525.6	527.0	528.4	529.8	531.2	532.7	534.1	535.5

TEMPERATURE VS. LATTICE PARAMETER FOR GOLD

Å	.0000	.0001	.0002	.0003	.0004	.0005	.0006	.0007	.0008	.0009
					DEGREES C					
4.111	536.9	538.3	539.7	541.1	542.5	543.9	545.3	546.7	548.0	549.4
4.112	550.8	552.2	553.6	555.0	556.4	557.8	559.2	560.6	562.0	563.3
4.113	564.7	566.1	567.5	568.9	570.3	571.6	573.0	574.4	575.8	577.2
4.114	578.5	579.9	581.3	582.7	584.0	585.4	586.8	588.2	589.5	590.9
4.115	592.3	593.6	595.0	596.4	597.7	599.1	600.5	601.8	603.2	604.6
4.116	605.9	607.3	608.6	610.0	611.4	612.7	614.1	615.4	616.8	618.1
4.117	619.5	620.8	622.2	623.5	624.9	626.2	627.6	628.9	630.3	631.6
4.118	633.0	634.3	635.7	637.0	638.4	639.7	641.0	642.4	643.7	645.1
4.119	646.4	647.7	649.1	650.4	651.7	653.1	654.4	655.8	657.1	658.4
4.120	659.7	661.1	662.4	663.7	665.1	666.4	667.7	669.0	670.4	671.7
4.121	673.0	674.3	675.7	677.0	678.3	679.6	680.9	682.3	683.6	684.9
4.122	686.2	687.5	688.8	690.2	691.5	692.8	694.1	695.4	696.7	698.0
4.123	699.3	700.7	702.0	703.3	704.6	705.9	707.2	708.5	709.8	711.1
4.124	712.4	713.7	715.0	716.3	717.6	718.9	720.2	721.5	722.8	724.1
4.125	725.4	726.7	728.0	729.3	730.6	731.9	733.2	734.4	735.7	737.0
4.126	738.3	739.6	740.9	742.2	743.5	744.8	746.0	747.3	748.6	749.9
4.127	751.2	752.5	753.7	755.0	756.3	757.6	758.9	760.1	761.4	762.7
4.128	764.0	765.2	766.5	767.8	769.1	770.3	771.6	772.9	774.2	775.4
4.129	776.7	778.0	779.2	780.5	781.8	783.0	784.3	785.6	786.8	788.1
4.130	789.4	790.6	791.9	793.1	794.4	795.7	796.9	798.2	799.4	800.7
4.131	802.0	803.2	804.5	805.7	807.0	808.2	809.5	810.7	812.0	813.2
4.132	814.5	815.7	817.0	818.2	819.5	820.7	822.0	823.2	824.5	825.7
4.133	827.0	828.2	829.5	830.7	832.0	833.2	834.4	835.7	836.9	838.2
4.134	839.4	840.6	841.9	843.1	844.3	845.6	846.8	848.1	849.3	850.5
4.135	851.8	853.0	854.2	855.4	856.7	857.9	859.1	860.4	861.6	862.8
4.136	864.1	865.3	866.5	867.7	869.0	870.2	871.4	872.6	873.9	875.1
4.137	876.3	877.5	878.7	880.0	881.2	882.4	883.6	884.8	886.1	887.3
4.138	888.5	889.7	890.9	892.1	893.3	894.6	895.8	897.0	898.2	899.4
4.139	900.6	901.8	903.0	904.2	905.5	906.7	907.9	909.1	910.3	911.5
4.140	912.7	913.9	915.1	916.3	917.5	918.7	919.9	921.1	922.3	923.5
4.141	924.7	925.9	927.1	928.3	929.5	930.7	931.9	933.1	934.3	935.5
4.142	936.7	937.9	939.1	940.3	941.5	942.6	943.8	945.0	946.2	947.4
4.143	948.6	949.8	951.0	952.2	953.4	954.5	955.7	956.9	958.1	959.3
4.144	960.5	961.6	962.8	964.0	965.2	966.4	967.6	968.7	969.9	971.1
4.145	972.3	973.5	974.6	975.8	977.0	978.2	979.3	980.5	981.7	982.9
4.146	984.0	985.2	986.4	987.6	988.7	989.9	991.1	992.2	993.4	994.6
4.147	995.8	996.9	998.1	999.3	1000.	1002.	1003.	1004.	1005.	1006.

APPENDIX II

PLATINUM VS. GOLD THERMOCOUPLE
DEGREES CENTIGRADE - REFERENCE JUNCTION 0 C

C	0	1	2	3	4	5	6	7	8	9
					MILLIVOLTS					
0	0.	0.006	0.012	0.018	0.024	0.031	0.037	0.043	0.049	0.056
10	0.062	0.068	0.075	0.081	0.088	0.094	0.101	0.108	0.114	0.121
20	0.128	0.134	0.141	0.148	0.155	0.162	0.169	0.176	0.183	0.190
30	0.197	0.204	0.211	0.218	0.225	0.233	0.240	0.247	0.255	0.262
40	0.269	0.277	0.284	0.292	0.299	0.307	0.314	0.322	0.330	0.337
50	0.345	0.353	0.361	0.369	0.376	0.384	0.392	0.400	0.408	0.416
60	0.424	0.432	0.441	0.449	0.457	0.465	0.473	0.482	0.490	0.498
70	0.507	0.515	0.524	0.532	0.540	0.549	0.558	0.566	0.575	0.583
80	0.592	0.601	0.610	0.618	0.627	0.636	0.645	0.654	0.663	0.672
90	0.680	0.690	0.699	0.708	0.717	0.726	0.735	0.744	0.753	0.763
100	0.772	0.781	0.790	0.800	0.809	0.819	0.828	0.838	0.847	0.857
110	0.866	0.876	0.885	0.895	0.905	0.914	0.924	0.934	0.944	0.953
120	0.963	0.973	0.983	0.993	1.003	1.013	1.023	1.033	1.043	1.053
130	1.063	1.073	1.083	1.093	1.104	1.114	1.124	1.134	1.145	1.155
140	1.165	1.176	1.186	1.197	1.207	1.218	1.228	1.239	1.249	1.260
150	1.271	1.281	1.292	1.303	1.313	1.324	1.335	1.346	1.357	1.367
160	1.378	1.389	1.400	1.411	1.422	1.433	1.444	1.455	1.466	1.477
170	1.488	1.500	1.511	1.522	1.533	1.544	1.556	1.567	1.578	1.590
180	1.601	1.612	1.624	1.635	1.647	1.658	1.670	1.681	1.693	1.705
190	1.716	1.728	1.739	1.751	1.763	1.775	1.786	1.798	1.810	1.822
200	1.834	1.845	1.857	1.869	1.881	1.893	1.905	1.917	1.929	1.941
210	1.953	1.965	1.977	1.990	2.002	2.014	2.026	2.038	2.051	2.063
220	2.075	2.088	2.100	2.112	2.125	2.137	2.149	2.162	2.174	2.187
230	2.199	2.212	2.225	2.237	2.250	2.262	2.275	2.288	2.300	2.313
240	2.326	2.339	2.351	2.364	2.377	2.390	2.403	2.416	2.428	2.441
250	2.454	2.467	2.480	2.493	2.506	2.519	2.532	2.546	2.559	2.572
260	2.585	2.598	2.611	2.625	2.638	2.651	2.664	2.678	2.691	2.704
270	2.718	2.731	2.744	2.758	2.771	2.785	2.798	2.812	2.825	2.839
280	2.852	2.866	2.880	2.893	2.907	2.920	2.934	2.948	2.962	2.975
290	2.989	3.003	3.017	3.031	3.044	3.058	3.072	3.086	3.100	3.114
300	3.128	3.142	3.156	3.170	3.184	3.198	3.212	3.226	3.240	3.254
310	3.268	3.283	3.297	3.311	3.325	3.340	3.354	3.368	3.382	3.397
320	3.411	3.425	3.440	3.454	3.469	3.483	3.498	3.512	3.526	3.541
330	3.556	3.570	3.585	3.599	3.614	3.628	3.643	3.658	3.672	3.687
340	3.702	3.717	3.731	3.746	3.761	3.776	3.791	3.805	3.820	3.835
350	3.850	3.865	3.880	3.895	3.910	3.925	3.940	3.955	3.970	3.985
360	4.000	4.015	4.030	4.045	4.061	4.076	4.091	4.106	4.121	4.137
370	4.152	4.167	4.183	4.198	4.213	4.229	4.244	4.259	4.275	4.290
380	4.306	4.321	4.336	4.352	4.367	4.383	4.399	4.414	4.430	4.445
390	4.461	4.477	4.492	4.508	4.524	4.539	4.555	4.571	4.587	4.602

PLATINUM VS. GOLD THERMOCOUPLE
DEGREES CENTIGRADE - REFERENCE JUNCTION 0 C

C	0	1	2	3	4	5	6	7	8	9
					MILLIVOLTS					
400	4.618	4.634	4.650	4.666	4.681	4.697	4.713	4.729	4.745	4.761
410	4.777	4.793	4.809	4.825	4.841	4.857	4.873	4.889	4.905	4.921
420	4.938	4.954	4.970	4.986	5.002	5.019	5.035	5.051	5.067	5.084
430	5.100	5.116	5.133	5.149	5.165	5.182	5.198	5.215	5.231	5.248
440	5.264	5.281	5.297	5.314	5.330	5.347	5.363	5.380	5.397	5.413
450	5.430	5.446	5.463	5.480	5.497	5.513	5.530	5.547	5.564	5.580
460	5.597	5.614	5.631	5.648	5.665	5.682	5.699	5.715	5.732	5.749
470	5.766	5.783	5.800	5.817	5.835	5.852	5.869	5.886	5.903	5.920
480	5.937	5.954	5.972	5.989	6.006	6.023	6.040	6.058	6.075	6.092
490	6.110	6.127	6.144	6.162	6.179	6.197	6.214	6.231	6.249	6.266
500	6.284	6.301	6.319	6.336	6.354	6.372	6.389	6.407	6.424	6.442
510	6.460	6.477	6.495	6.513	6.530	6.548	6.566	6.584	6.601	6.619
520	6.637	6.655	6.673	6.691	6.709	6.726	6.744	6.762	6.780	6.798
530	6.816	6.834	6.852	6.870	6.888	6.906	6.925	6.943	6.961	6.979
540	6.997	7.015	7.033	7.052	7.070	7.088	7.106	7.125	7.143	7.161
550	7.179	7.198	7.216	7.235	7.253	7.271	7.290	7.308	7.327	7.345
560	7.364	7.382	7.401	7.419	7.438	7.456	7.475	7.493	7.512	7.531
570	7.549	7.568	7.587	7.605	7.624	7.643	7.662	7.680	7.699	7.718
580	7.737	7.756	7.774	7.793	7.812	7.831	7.850	7.869	7.888	7.907
590	7.926	7.945	7.964	7.983	8.002	8.021	8.040	8.059	8.078	8.097
600	8.117	8.136	8.155	8.174	8.193	8.212	8.232	8.251	8.270	8.290
610	8.309	8.328	8.348	8.367	8.386	8.406	8.425	8.445	8.464	8.483
620	8.503	8.522	8.542	8.561	8.581	8.601	8.620	8.640	8.659	8.679
630	8.699	8.718	8.738	8.758	8.777	8.797	8.817	8.837	8.856	8.876
640	8.896	8.916	8.936	8.956	8.976	8.995	9.015	9.035	9.055	9.075
650	9.095	9.115	9.135	9.155	9.175	9.195	9.215	9.235	9.255	9.276
660	9.296	9.316	9.336	9.356	9.376	9.397	9.417	9.437	9.457	9.478
670	9.498	9.518	9.539	9.559	9.579	9.600	9.620	9.641	9.661	9.682
680	9.702	9.723	9.743	9.764	9.784	9.805	9.825	9.846	9.867	9.887
690	9.908	9.929	9.949	9.970	9.991	10.011	10.032	10.053	10.074	10.094
700	10.115	10.136	10.157	10.178	10.199	10.220	10.241	10.261	10.282	10.303
710	10.324	10.345	10.366	10.387	10.408	10.430	10.451	10.472	10.493	10.514
720	10.535	10.556	10.578	10.599	10.620	10.641	10.662	10.684	10.705	10.726
730	10.748	10.769	10.790	10.812	10.833	10.855	10.876	10.897	10.919	10.940
740	10.962	10.983	11.005	11.026	11.048	11.070	11.091	11.113	11.134	11.156
750	11.178	11.199	11.221	11.243	11.265	11.286	11.308	11.330	11.352	11.373
760	11.395	11.417	11.439	11.461	11.483	11.505	11.527	11.549	11.571	11.593
770	11.615	11.637	11.659	11.681	11.703	11.725	11.747	11.769	11.791	11.813
780	11.836	11.858	11.880	11.902	11.924	11.947	11.969	11.991	12.014	12.036
790	12.058	12.081	12.103	12.125	12.148	12.170	12.193	12.215	12.238	12.260

PLATINUM VS. GOLD THERMOCOUPLE
DEGREES CENTIGRADE - REFERENCE JUNCTION 0 C

C	0	1	2	3	4	5	6	7	8	9
					MILLIVOLTS					
800	12.283	12.305	12.328	12.350	12.373	12.396	12.418	12.441	12.463	12.486
810	12.509	12.532	12.554	12.577	12.600	12.623	12.645	12.668	12.691	12.714
820	12.737	12.760	12.782	12.805	12.828	12.851	12.874	12.897	12.920	12.943
830	12.966	12.989	13.012	13.035	13.058	13.082	13.105	13.128	13.151	13.174
840	13.197	13.221	13.244	13.267	13.290	13.314	13.337	13.360	13.384	13.407
850	13.430	13.454	13.477	13.501	13.524	13.547	13.571	13.594	13.618	13.641
860	13.665	13.689	13.712	13.736	13.759	13.783	13.807	13.830	13.854	13.878
870	13.901	13.925	13.949	13.973	13.996	14.020	14.044	14.068	14.092	14.116
880	14.139	14.163	14.187	14.211	14.235	14.259	14.283	14.307	14.331	14.355
890	14.379	14.403	14.427	14.451	14.475	14.500	14.524	14.548	14.572	14.596
900	14.621	14.645	14.669	14.693	14.718	14.742	14.766	14.791	14.815	14.839
910	14.864	14.888	14.912	14.937	14.961	14.986	15.010	15.035	15.059	15.084
920	15.108	15.133	15.158	15.182	15.207	15.231	15.256	15.281	15.305	15.330
930	15.355	15.380	15.404	15.429	15.454	15.479	15.503	15.528	15.553	15.578
940	15.603	15.628	15.653	15.678	15.703	15.728	15.753	15.778	15.803	15.828
950	15.853	15.878	15.903	15.928	15.953	15.978	16.003	16.029	16.054	16.079
960	16.104	16.129	16.154	16.180	16.205	16.230	16.256	16.281	16.306	16.332
970	16.357	16.382	16.408	16.433	16.459	16.484	16.510	16.535	16.561	16.586
980	16.612	16.637	16.663	16.688	16.714	16.739	16.765	16.791	16.816	16.842
990	16.868	16.893	16.919	16.945	16.971	16.996	17.022	17.048	17.074	17.100
1000	17.126									

APPENDIX III

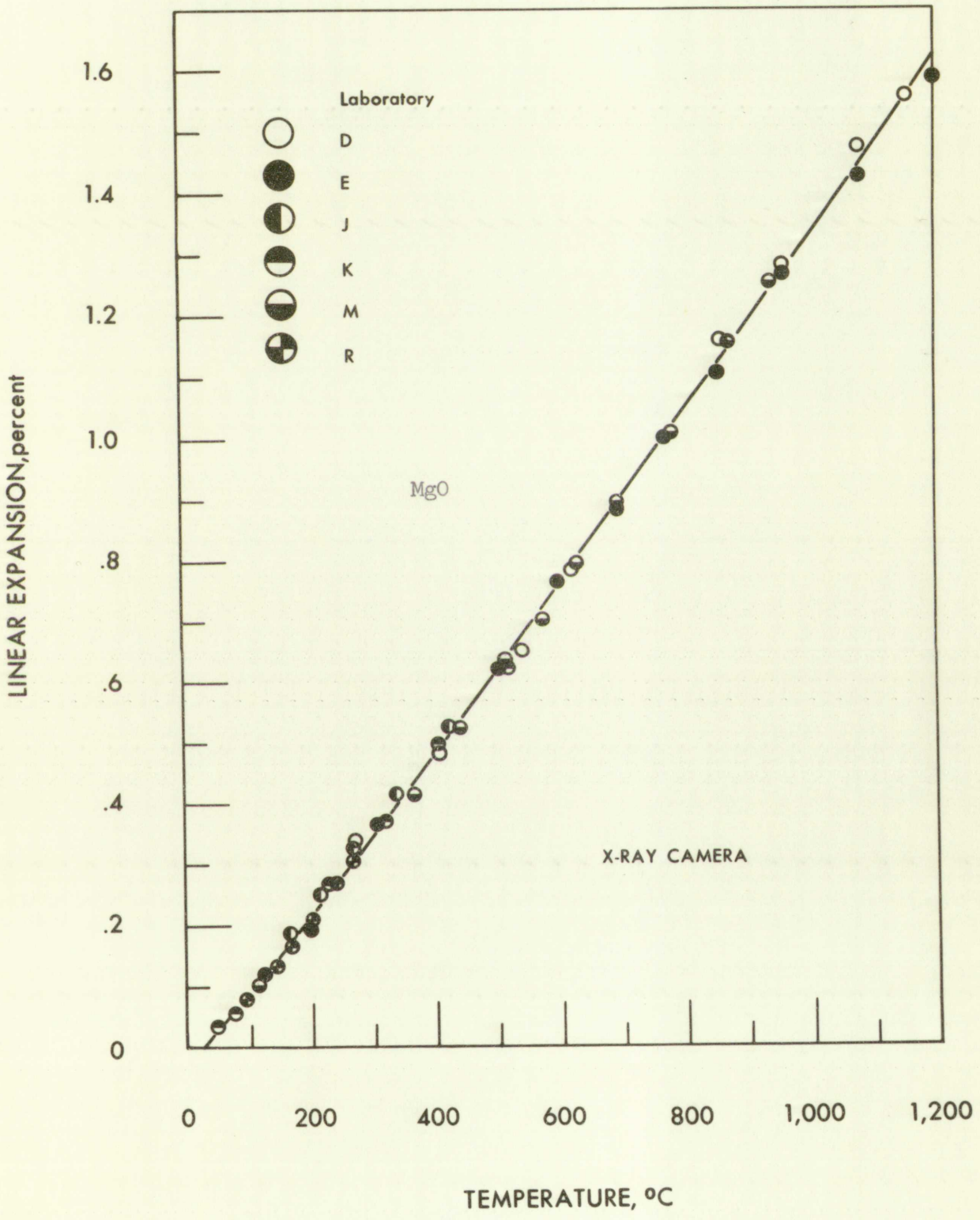

Results obtained by X-ray cameras in the Interlaboratory Study on Thermal Expansion of MgO. (Courtesy of Dr. W. J. Campbell and the Bureau of Mines)

APPENDIX IV

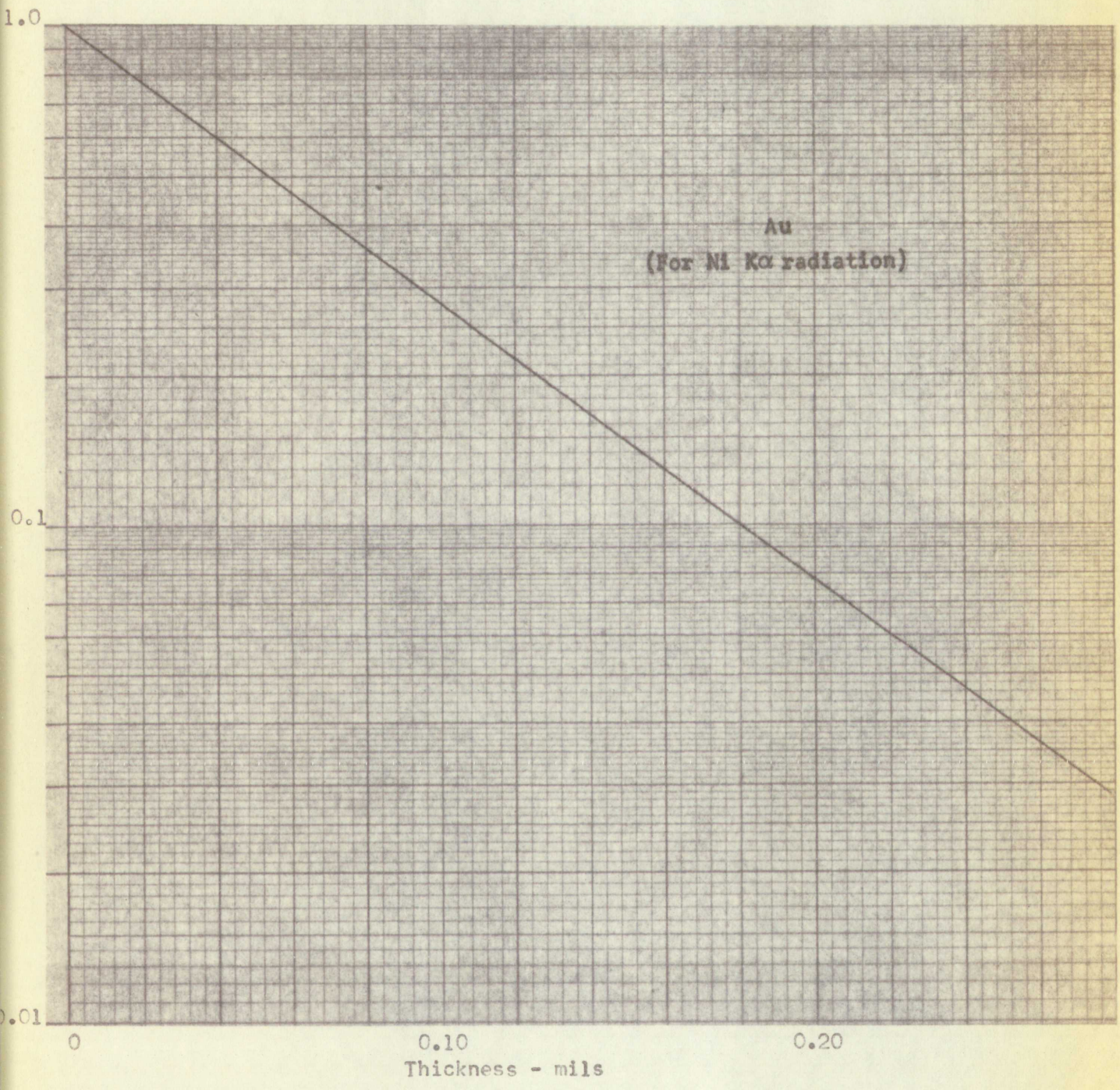

The attenuation of X-rays vs. the thickness of Au.

APPENDIX V

LIST OF SYMBOLS

A	area
$\overset{o}{A}$	Angstrom unit
Au	gold
a	lattice parameter
C	circumference
D	diameter of Debye-Scherrer camera
D, E	unknown constants
d	interplanar spacing
E	maximum error
f	shape factor
h, k, l	Miller indices
k	thermal conductivity
$K\alpha$	designation of line in diffraction pattern
MgO	magnesium oxide
Ni	nickel target
r	$\sqrt{\frac{k_t}{k_s}}$
S	ring diameter of diffraction cone
T	temperature, ^{o}K
t	temperature, ^{o}C